PLOS COMPUTATIONAL BIOLOGY

RESEARCH ARTICLE

Interactions between calmodulin and neurogranin govern the dynamics of CaMKII as a leaky integrator

Mariam Ordyan[1,2], **Tom Bartol**[2], **Mary Kennedy**[3], **Padmini Rangamani**[4]*, **Terrence Sejnowski**[1,2]*

1 Institute for Neural Computation, University of California San Diego, La Jolla, California, United States of America, **2** Computational Neurobiology Laboratory, Salk Institute for Biological Sciences, La Jolla, California, United States of America, **3** The Division of Biology and Biological Engineering, California Institute of Technology, Pasadena, California, United States of America, **4** Department of Mechanical and Aerospace Engineering, University of California San Diego, La Jolla, California, United States of America

* prangamani@ucsd.edu (PR), terry@salk.edu (TS)

Citation: Ordyan M, Bartol T, Kennedy M, Rangamani P, Sejnowski T (2020) Interactions between calmodulin and neurogranin govern the dynamics of CaMKII as a leaky integrator. PLoS Comput Biol 16(7): e1008015. https://doi.org/10.1371/journal.pcbi.1008015

Editor: Joanna Jędrzejewska-Szmek, Instytut Biologii Doswiadczalnej im M Nenckiego Polskiej Akademii Nauk, POLAND

Received: December 10, 2019

Accepted: June 4, 2020

Published: July 17, 2020

Peer Review History: PLOS recognizes the benefits of transparency in the peer review process; therefore, we enable the publication of all of the content of peer review and author responses alongside final, published articles. The editorial history of this article is available here: https://doi.org/10.1371/journal.pcbi.1008015

Data Availability Statement: All bngl files are available on GitHub at the following repository:

Abstract

Calmodulin-dependent kinase II (CaMKII) has long been known to play an important role in learning and memory as well as long term potentiation (LTP). More recently it has been suggested that it might be involved in the time averaging of synaptic signals, which can then lead to the high precision of information stored at a single synapse. However, the role of the scaffolding molecule, neurogranin (Ng), in governing the dynamics of CaMKII is not yet fully understood. In this work, we adopt a rule-based modeling approach through the Monte Carlo method to study the effect of Ca^{2+} signals on the dynamics of CaMKII phosphorylation in the postsynaptic density (PSD). Calcium surges are observed in synaptic spines during an EPSP and back-propagating action potential due to the opening of NMDA receptors and voltage dependent calcium channels. Using agent-based models, we computationally investigate the dynamics of phosphorylation of CaMKII monomers and dodecameric holoenzymes. The scaffolding molecule, Ng, when present in significant concentration, limits the availability of free calmodulin (CaM), the protein which activates CaMKII in the presence of calcium. We show that Ng plays an important modulatory role in CaMKII phosphorylation following a surge of high calcium concentration. We find a non-intuitive dependence of this effect on CaM concentration that results from the different affinities of CaM for CaMKII depending on the number of calcium ions bound to the former. It has been shown previously that in the absence of phosphatase, CaMKII monomers integrate over Ca^{2+} signals of certain frequencies through autophosphorylation (Pepke et al, Plos Comp. Bio., 2010). We also study the effect of multiple calcium spikes on CaMKII holoenzyme autophosphorylation, and show that in the presence of phosphatase, CaMKII behaves as a leaky integrator of calcium signals, a result that has been recently observed *in vivo*. Our models predict that the parameters of this leaky integrator are finely tuned through the interactions of Ng, CaM, CaMKII, and PP1, providing a mechanism to precisely control the sensitivity of synapses to calcium signals. Author Summary not valid for PLOS ONE submissions.

https://github.com/marordyan/CaMKII_well_mixed/.

Funding: PR,MO,TB,TS: FA9550-18-1-0051 US Air Force https://www.airforce.com/, TB,TS: P41GM103712 National Institute of Health https://www.nih.gov/ MK,TB,TS: NS44306MK National Institute of Health https://www.nih.gov/ MK,TB,TS: DA030749 National Institute of Health https://www.nih.gov/ The funders had no role in study design, data collection and analysis, decision to publish, or preparation of the manuscript.

Competing interests: The authors have declared that no competing interests exist.

Author summary

Neurons communicate with each other through synapses. The strength of a particular synapse is effectively the level of sensitivity of the postsynaptic neuron in response to firing of the presynaptic neuron. The process of changing synaptic strength is dubbed synaptic plasticity, a foundational aspect of learning and memory. In this work, we create a computational model of a calcium signaling pathway that sets off a chain reaction in CaMKII phosphorylation, eventually leading to synaptic plasticity. Computational modeling provides a unique way to tease apart and understand the non-intuitive results of interactions between the molecules involved. Our model successfully predicts the experimentally observed activation dynamics of this crucially important enzyme which is necessary for learning. These dynamics, along with other pathways, regulate the size of the synapse, which is known to be highly correlated with synaptic strength. In this work, we reveal quantitative characteristics of CaMKII activation for various stimuli, leading to important insights regarding the potential role of Neurogranin, a scaffolding protein in this pathway.

Introduction

Information is stored in the brain through synaptic plasticity. It has been reported that synaptic strength is highly correlated with the size of the spine head, and the precision of information stored at a single synapse is quite high despite the stochastic variability of synaptic activation [1–3]. Structural changes to the postsynaptic spine that can lead to spine enlargement, and thus structural plasticity are triggered by Ca^{2+} signaling [4, 5]. Time averaging of these calcium signals has been suggested as a plausible mechanism for achieving the high precision of information processing observed in spines. Furthermore, phosphorylation of calcium/calmodulin-dependent protein kinase II (CaMKII) has been postulated as the most probable pathway satisfying the long time scales predicted for averaging [1].

CaMKII is an autophosphorylating kinase [6, 7] [8–10]; in postsynaptic densities (PSD), CaMKII has been shown to play an important role in learning and memory [11]. Specifically, mice with a mutation in a subtype of CaMKII exhibit deficiencies in long-term potentiation (LTP) and spatial learning [10, 12, 13]. Moreover, CaMKII expression regulates the rate of dendritic arborization and the branch dynamics [14, 15], highlighting its importance in structural plasticity. Additionally, CaMKII has been shown to bind actin, the major cytoskeletal protein in dendritic spines [16–18], further emphasizing its role in structural plasticity. Activation of CaMKII is exquisitely regulated at multiple levels as summarized below.

- **CaMKII activation by calmodulin (CaM)**: CaMKII is activated by calmodulin (CaM) [6], which is a protein with 4 Ca^{2+} binding sites: 2 on its C-terminal and 2 on N-terminal (Fig 1A) [19, 20]. CaM binds Ca^{2+} cooperatively and is able to activate CaMKII more potently if it has more Ca^{2+} ions bound to it [21].
- **Neurogranin (Ng)-CaM interactions**: In the absence of Ca^{2+}, CaM is bound to scaffolding protein neurogranin (Ng), which dramatically reduces the affinity of CaM for Ca^{2+} (Fig 1B). On the other hand, Ca^{2+} decreases binding affinity of CaM for Ng [22]. Thus, CaM activation and therefore CaMKII activation depend on the competitive effects of Ca^{2+} and Ng.
- **The role of structure in CaMKII activation**: Further complexity for CaMKII activation is built into the structure of the molecule itself. CaMKII is a dodecamer arranged in 2 stacked hexomeric rings [6, 23]. Monomers of CaMKII truncated to remove the association domain

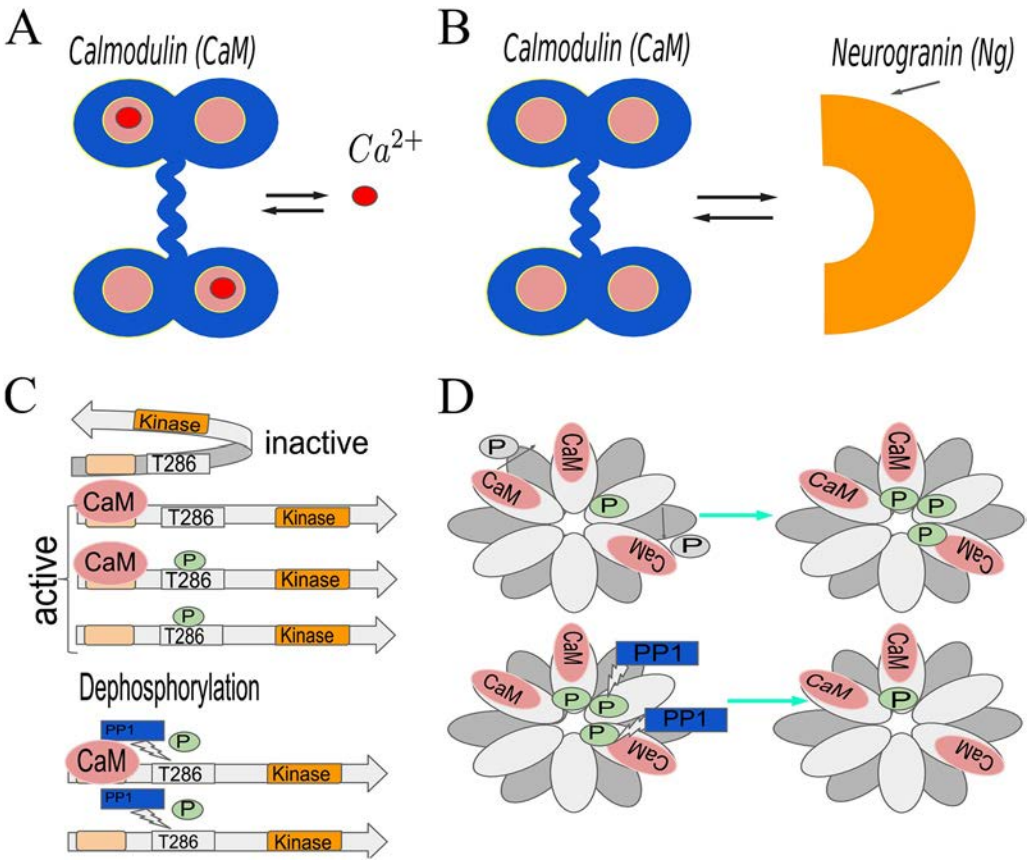

Fig 1. Schematic representation of the interactions between calmodulin (CaM), calcium, CaMKII, and neurogranin (Ng). (A) Calmodulin has 4 calcium binding sites; it binds Ca^{2+} cooperatively and its ability to activate CaMKII depends on how many of these sites are occupied. (B) Neurogranin (Ng) is a scaffolding molecule; upon binding calmodulin it dramatically reduces the latter's affinity for calcium. In this work, we assume that CaM cannot bind calcium and Ng simultaneously. (C) The default conformation of CaMKII monomers is inactive (top); they can be activated by CaM binding. Once bound to CaM, the monomers can be phosphorylated by another active CaMKII protein. In this case, the CaMKII monomer will remain active even after losing CaM. Protein phosphatase 1 (PP1) dephosphorylates CaMKII (bottom). (D) CaMKII holoenzyme is a dodecamer, which consists of 2 stacked hexomeric rings of CaMKII monomers. Within the ring, a given CaMKII monomer can be phosphorylated by its neighbor provided that they are both in the active conformation. This is commonly referred to as autophosphorylation.

https://doi.org/10.1371/journal.pcbi.1008015.g001

(mCaMKII) contain a kinase domain, CaM-binding domain, and phosphorylation sites T286 (287), and T305(306) [9, 24–26]. When the CaM-binding domain is unoccupied, and the T286(287) site is unphosphorylated, the monomer is in a conformation such that the kinase is inactive (Fig 1C, top). When CaM is bound to a CaMKII monomer, the latter undergoes a conformational change, such that the kinase is now active. An active CaMKII monomer can phosphorylate other Ca^{2+}/*CaM*-bound CaMKII monomers resulting in CaMKII autophosphorylation. A CaMKII monomer can only be phosphorylated if the calmodulin bound to it has at least one calcium ion, and once phosphorylated [27], the monomer remains in the active state even after unbinding from CaM (Fig 1C middle). The same is true for full length monomers that are bound within the holoenzyme. In this manner, a brief Ca^{2+} influx initiates a prolonged CaMKII activation [7, 9, 26, 27, 27–29]. Within the holoenzyme each of the monomers can phosphorylate neighbors, as long as the former is active and the latter has CaM bound to it (Fig 1D) [8, 27]. The phosphorylation rate of the CaMKII monomers depends on how many Ca^{2+} ions are bound to the CaM bound to that substrate [30].

- **Phosphatases are important**: Various types of protein phosphatases (PP1, PP2A, PP2B, PP2C) can dephosphorylate CaMKII in the brain and, if CaM is not bound to the latter, bring it back to its inactive state [25, 31]. In the PSD, however, protein phosphatase 1 (PP1) has been shown to be mainly responsible for CaMKII dephosphorylation [31, 32] (Fig 1C bottom).

Many computational models of CaMKII dynamics have been developed in the literature to probe the different interactions in this cascade at varying levels of detail [11, 33–40]. A large majority of these models focused on the bistability behavior of CaMKII [11, 33, 35, 37, 38, 40], which resulted from the nonlinear rate functions used in the model. However, experiments suggest that in long-term potentiation, CaMKII is only transiently activated and does not exhibit bistable behavior [41, 42]. Furthermore, as noted recently [43], the behavior of CaMKII is complicated by its multimeric nature and by the intersubunit interaction necessary for phosphorylation of T286, which is affected by the presence of Ng and protein phosphatases. Therefore, a more complete computational model of CaMKII dynamics needs to account for both the behavior of the monomers and the dynamics of CaMKII holoenzyme in the presence of Ng and PP1.

Here we sought to examine how the competition between Ca^{2+}-mediated activation of CaM and Ng scaffolding of CaM affects the response of CaMKII to calcium signals. To do so, we developed two computational models—Model 1 that accounts for CaMKII monomer activation and Model 2 that investigates holoenzyme kinetics—in an agent-based framework. Model 1 is built on a previously published model of activation of CaMKII monomers by Ca^{2+}/CaM [30] and now includes the role of the scaffolding molecule Ng and the protein phosphatase PP1. Using these models we investigated the dynamics of monomeric and dodecameric CaMKII phosphorylation as a function of the dynamics of Ca^{2+}-influx and of interactions with Ng. An important distinction between our model and those presented in [34] and [44] is that we did not explicitly construct our model to replicate desired/observed CaMKII activation dynamics. Rather, our model hinges solely on rate constants for interactions between molecules based on biochemical experiments and presented in Tables 1 and 2. Our results show that under conditions of our model CaMKII behaves as a leaky integrator and, more importantly, that the scaffold molecule, Ng, tunes the behavior of this leaky integrator.

Methods

We constructed the models at different scales to characterize CaMKII phosphorylation at increasing levels of complexity. First, we added the scaffolding molecule Ng to the model from *Pepke et al* [30], to investigate the effect of Ng on CaMKII phosphorylation dynamics. Second, we added PP1 to this CaMKII monomers model to simulate the phosphorylation-dephosphorylation cycle and characterize the effects of Ng on this system. Finally, we built a model of a dodecameric holoenzyme and looked at the response of the holoenzyme-phosphatase system to calcium signals and how it is affected by Ng. An important assumption of all the models developed in this study is that only one of the phosphorylation sites (T286/7) of CaMKII is considered throughout. The phosphorylation of T305/6 site is a slower reaction that is known to inhibit CaM binding to T286/7-unphosphorylated CaMKII subunit [114], and is omitted from our simulations.

Model description

Model of CaMKII monomers. We begin with the model of CaMKII monomers (mCaMKII) described by Pepke et al. [30]. This model includes Ca^{2+} binding rates to CaM, CaM

Table 1. Reaction rates for the model.

Description	Parameter	Value	Reference	Parameter	Value	Reference
Ca^{2+} binding to CaM	k_{on}^{1C}	4 $\mu M^{-1}s^{-1}$	[21, 30, 45, 46]	k_{off}^{1C}	40.24 s^{-1}	[47–49]
	k_{on}^{2C}	10 $\mu M^{-1}s^{-1}$	[21, 30, 45, 46]	k_{off}^{2C}	9.3 s^{-1}	[49]
	k_{on}^{1N}	100 $\mu M^{-1}s^{-1}$	[21, 30, 45, 46]	k_{off}^{1N}	2660 s^{-1}	[47, 49–51]
	k_{on}^{2N}	150 $\mu M^{-1}s^{-1}$	[21, 30, 45, 46]	k_{off}^{2N}	990 s^{-1}	[47–51]
CaM binding to unphosphorylated CaMKII	k_{on}^{CaM0}	$3.8 \cdot 10^{-3}$ M -1 s -1	[30, 52]	k_{off}^{CaM0}	6.56 s^{-1}	[30, 52]
	k_{on}^{CaM1C}	$59 \cdot 10^{-3}$ $\mu M^{-1}s^{-1}$	[30, 52]	k_{off}^{CaM1C}	6.72 s^{-1}	[30, 52]
	k_{on}^{CaM2C}	0.92 $\mu M^{-1}s^{-1}$	[30, 52]	k_{off}^{CaM2C}	6.35 s^{-1}	[30, 52]
	$k_{on}^{CaM1C1N}$	0.33 $\mu M^{-1}s^{-1}$	[30, 52]	$k_{off}^{CaM1C1N}$	5.68 s^{-1}	[30, 52]
	$k_{on}^{CaM2C1N}$	5.2 $\mu M^{-1}s^{-1}$	[30, 52]	$k_{off}^{CaM2C1N}$	5.25 s^{-1}	[30, 52]
	k_{on}^{CaM1N}	$22 \cdot 10^{-3}$ $\mu M^{-1}s^{-1}$	[30, 52]	k_{off}^{CaM1N}	5.75 s^{-1}	[30, 52]
	k_{on}^{CaM2N}	0.1 $\mu M^{-1}s^{-1}$	[30, 52]	k_{off}^{CaM2N}	1.68 s^{-1}	[30, 52]
	$k_{on}^{CaM1C2N}$	1.9 $\mu M^{-1}s^{-1}$	[30, 52]	$k_{off}^{CaM1C2N}$	2.09 s^{-1}	[30]
	k_{on}^{CaM4}	30 $\mu M^{-1}s^{-1}$	[30, 52]	k_{off}^{CaM4}	1.95 s^{-1}	[30, 52]
Ca^{2+} binding to CaM-CaMKII	k_{on}^{K1C}	44 $\mu M^{-1}s^{-1}$	[30, 49]	k_{off}^{K1C}	29.04 s^{-1}	[30, 49]
	k_{on}^{K2C}	44 $\mu M^{-1}s^{-1}$	[30, 49]	k_{off}^{K2C}	2.42 s^{-1}	[30, 49]
	k_{on}^{K1N}	75 $\mu M^{-1}s^{-1}$	[30, 49]	k_{off}^{K1N}	301.5 s^{-1}	[30, 49]
	k_{on}^{K2N}	76 $\mu M^{-1}s^{-1}$	[30, 49]	k_{off}^{K2N}	32.68 s^{-1}	[30, 49]
CaMKII binding to CaM-CaMKII *	k_{on}^{CaMKII}	50 $\mu M^{-1}s^{-1}$	[30, 53]	k_{off}^{CaMKII}	60 s^{-1}	[27, 30, 54]
CaMKII phosphorylation	k_{p}^{CaM1C}	0.032 s^{-1}	[21, 30]	k_{p}^{CaM2C}	0.064 s^{-1}	[21, 30]
	$k_{p}^{CaM1C1N}$	0.094 s^{-1}	[21, 30]	$k_{p}^{CaM2C1N}$	0.124 s^{-1}	[21, 30]
	k_{p}^{CaM1N}	0.061 s^{-1}	[21, 30]	k_{p}^{CaM2N}	0.12 s^{-1}	[21, 30]
	$k_{p}^{CaM1C2N}$	0.154 s^{-1}	[21, 30]	k_{p}^{CaM4}	0.96 s^{-1}	[21, 30]
CaM binding to phosphorylated CaMKII	$k_{p,on}^{CaM0}$	$1.27 \cdot 10^{-3}$ $\mu M^{-1}s^{-1}$	[30, 52]	$k_{p,on}^{CaM1C}$	19.7 $\mu M^{-1}s^{-1}$	[30, 52]
	$k_{p,on}^{CaM2C}$	0.3 $\mu M^{-1}s^{-1}$	[30, 52]	$k_{p,on}^{CaM1C1N}$	1.1 $\mu M^{-1}s^{-1}$	[30, 52]
	$k_{p,on}^{CaM2C1N}$	1.73 $\mu M^{-1}s^{-1}$	[30, 52]	$k_{p,on}^{CaM1N}$	7.3 $\mu M^{-1}s^{-1}$	[30, 52]
	$k_{p,on}^{CaM2N}$	0.03 $\mu M^{-1}s^{-1}$	[30, 52]	$k_{p,on}^{CaM1C2N}$	0.63 $\mu M^{-1}s^{-1}$	[30, 52]
	$k_{p,on}^{CaM4}$	10 $\mu M^{-1}s^{-1}$	[30, 52]	$k_{p,off}^{CaM}$	0.07 s^{-1}	[52]
Ng binding to CaM	k_{on}^{Ng}	5 $\mu M^{-1}s^{-1}$	[55]	k_{off}^{Ng}	1 s^{-1}	[55]
CaMKII dephosphorylation by PP1 (Michaelis-Menten constants)	k_{cat}	0.41 s^{-1}	[56]	K_m	11 μM	[56]

All the numbers with the exception of "CaMKII binding to CaM-CaMKII" are used in both monomers and holoenzyme models. The difference between the 2 models are the initial conditions: we either start the simulations with only monomers or only holoenzyme, and do not allow the disintegration of the latter.

* only present in the model for monomers

https://doi.org/10.1371/journal.pcbi.1008015.t001

binding rates to mCaMKII, and phosphorylation rates of active CaMKII monomers by one another, all depending on how many Ca^{2+} ions are bound to the CaM molecules involved. We incorporate Ng binding to CaM with the rate constants from [55], and assume that the binding of CaM to Ca^{2+} and Ng is mutually exclusive (Table 1). In addition to the reactions in [30], we included CaM unbinding and binding to phosphorylated CaMKII, albeit with slower kinetics [52]. This reaction is important for the timescales of our interest (on the order of minutes) and we adapt these reaction rates from [52]. Finally, CaMKII dephosphorylation by PP1 is modeled as Michaelis-Menten kinetics, with the rate constants from [56] (Table 1).

Table 2. Reactions implemented in our models.

$Ca^{2+} + CaM((n-1)Ca^{2+}) \underset{k^{n}_{off}}{\overset{k^{n}_{on}}{\rightleftharpoons}} CaM(nCa^{2+})$
$Ng + CaM(0Ca^{2+}) \underset{k^{ng}_{off}}{\overset{k^{ng}_{on}}{\rightleftharpoons}} CaM \cdot Ng$
$CaMKII + CaM(nCa^{2+}) \underset{k^{CaMnCa}_{off}}{\overset{k^{CaMnCa}_{on}}{\rightleftharpoons}} CaMKII \cdot CaM(nCa^{2+})$
$CaMKII \cdot CaM((n-1)Ca^{2+}) + Ca^{2+} \underset{k^{KnCa}_{off}}{\overset{k^{KnCa}_{on}}{\rightleftharpoons}} CaMKII \cdot CaM(nCa^{2+})$
$CaMKII \cdot CaM(nCa^{2+}) + CaMKII \cdot CaM(mCa^{2+}) \underset{k^{CaMKII}_{off}}{\overset{k^{CaMKII}_{on}}{\rightleftharpoons}} CaMKII \cdot CaM(nCa^{2+}) \cdot CaMKII \cdot CaM(mCa^{2+})$
$CaMKII \cdot CaM(nCa^{2+}) \cdot CaMKII \cdot CaM(mCa^{2+}) \xrightarrow{k^{CaMmCa}_{p}} CaMKII \cdot CaM(nCa^{2+}) \cdot pCaMKII \cdot CaM(mCa^{2+})$
$pCaMKII \cdot CaM(nCa^{2+}) \underset{k^{CaMnCa}_{p,on}}{\overset{k^{CaM}_{p,off}}{\rightleftharpoons}} pCaMKII + CaM(nCa^{2+})$
$PP_1 + pCaMKII \cdot CaM(nCa^{2+}) \overset{k_M}{\rightleftharpoons} PP_1 \cdot pCaMKII \cdot CaM(nCa^{2+}) \xrightarrow{k_{cat}} PP_1 + CaMKII \cdot CaM(nCa^{2+})$

Listed are the reactions implemented in both models with the exception of the 5th reaction between 2 CaMKII monomers, that is only present in the mCaMKII model since in the hCaMKII model the the subunits are already linked to one another within the holoenzyme. Here n stands for the number and different configurations of Ca^{2+} ions bound to CaM (thus nCa^{2+} should be read as 'aCbN', where a and b can range from 0 to 2, see Table 1.)

https://doi.org/10.1371/journal.pcbi.1008015.t002

Model of CaMKII holoenzyme. **Assumptions specific to the holoenzyme model**: It has been shown that while the kinase domains of individual subunits are attached to the rigid hub domain with a highly flexible linker domain, ∼20% of subunits form dimers, and ∼ 3% of them are in a compact conformation, both of which render CaM-binding-domain inaccessible [115]. Here, we do not include such detailed interactions between linker domains and flexibility of the individual subunits within the holoenzyme. Rather, we assume that the kinase domains are positioned rigidly within the 2 hexameric rings, such that each subunit is in a position to phosphorylate only one of its neighbors as depicted in Fig 1D.

We further assume that the CaMKII subunits within the holoenzyme have the same binding rates to different species of Ca^{2+}/CaM as the CaMKII monomers, and once activated their phosphorylation rate is the same as that of the corresponding monomers. Any possible

allosteric interactions are ignored. Based on these assumptions, the model for the CaMKII holoenzyme does not include the reaction for 2 CaMKII monomers binding to one another. Rather, once the appropriate neighbor of an active CaMKII subunit binds Ca^{2+}/CaM, the phosphorylation rule is invoked with the corresponding reaction rate (Table 1).

Model development. To model the dynamics of CaMKII holoenzyme, we changed the types of molecules that we start the simulation with. Instead of CaMKII monomers, we initiated the simulation with CaMKII holoenzymes, and defined the phosphorylation rules for individual subunits such that a given subunit can only phosphorylate one of its neighbors (see model assumptions). The rules are the same as those of the monomers, with the exception of 2 CaMKII monomers binding each other to phosphorylate one another, since they are already bound within the holoenzyme. In this case, the reaction rules apply to the CaMKII subunits within the holoenzyme rather than CaMKII monomers.

This model does not contain any CaMKII monomers outside of the holoenzyme. We calculated the total number of the holoenzymes to keep the concentration of the $[mCaMKII] = 80\ \mu M$ consistent with our model of the monomers. For our simulated PSD volume $V = 0.0156\ \mu m^3$ this concentration corresponds to $80\ \mu M = 80 \cdot (6.022 \cdot 10^{23} \cdot 0.0156 \cdot 10^{-15}) \cdot 10^{-6}$ monomers which constitutes $752/12 \approx 63$ holoenzymes.

Rule-based modeling and BioNetGen

Since each CaMKII monomer can bind a calmodulin molecule, which can adopt 9 distinct states (assuming that the 2 Ca^{2+} binding sites on each of the lobes are indistinguishable), and be phosphorylated or unphosphorylated, there are more than 18^{12} states the dodecameric holoenzyme could adopt. To avoid a combinatorial explosion of states we built our model in a rule-based modeling language BioNetGen [116], which is briefly described here.

A powerful idea at the heart of rule-based modeling is colloquially referred as "don't care, don't write" [117, 118]. Here, for a given reaction (or rule), we only specify the states of the reactants that are relevant for the said reaction, and leave the rest unspecified. For example, a specific CaMKII subunit will bind a given species of Ca^{2+}/CaM with the same rate regardless of the conformation of its neighbors. Thus, a rule to bind a CaM molecule that has 2 Ca^{2+} ions bound to its C-terminus would look like:

$CaMKII(286 \sim U, cam) + CaM(camkii, C \sim 2, N \sim 0) \Longleftrightarrow CaMKII(286 \sim U, cam!1).CaM(camkii!1, C \sim 2, N \sim 0), k_{on}^{CaM2C},\ k_{off}^{CaM2C}$.

This rule indicates that regardless of the presence or conformations of a non-phosphorylated (indicated by $286 \sim U$) CaMKII subunits' neighbors it binds CaM, with 2 Ca^{2+} ions at its C lobe, reversibly with the reaction rates k_{on}^{CaM2C} and k_{off}^{CaM2C} (Table 1). This dramatically reduces the number of reactions that need to be written. In the case of our CaMKII model, we only end up with ~ 40 reactions despite the huge number of possible states.

In BioNetGen, once the reactions have been specified, if there is no danger of running into combinatorial explosion (the numbers of possible states and reactions are manageable), a full network of reactions can be generated, and the simulations can be run with ordinary differential equations (ODEs) [118]. If the number of states of a given enzyme is too large however, a stochastic agent-based approach is adopted, in which case only the reactions between existing discrete molecules that occur during the simulation need to be tracked by the program (network free simulation [119, 120]). In this case, the important quantity is the number of different states present which can be much smaller than the number of possible states. In this work, we conduct the simulations for the monomer model with ODEs, and for the holoenzyme model with the network free method.

Modeling calcium inputs

To implement Ca^{2+} pulses, we needed to include time-dependent rate constants into our model. For this purpose we concocted the following reaction:

$$0 \Rightarrow t(), ticspersecond$$

This allowed us to implement a reaction with a rate constant dependent on t(), namely a Ca^{2+} pulse:

$$0 \Rightarrow Ca, \ \ A * (t()/\tau_R) * e^{-(t()/\tau_F)}$$

where A, τ_R, and τ_F are the amplitude, and the raising and falling time constants of the reaction rate (see the model). These parameters where chosen such as to produces the desired shapes of the Ca^{2+}_{free} pulses.

Results

Distribution of different calcium-bound CaM depends on the presence or absence of Ng. We assumed that all molecules were well mixed and adopted a rule-based Monte Carlo approach to simulate the reaction dynamics (see Methods). Since Ng is a scaffolding molecule and its presence is expected to decrease the $[CaM]_{free}$: $[Ca^{2+}]_{free}$ ratio we first investigated how it affects the distribution of different calcium-bound CaM molecules while maintaining $[Ca^{2+}]$ constant. Following Pepke *et al.* [30], we set $[mCaMKII]$ = 80 μM and calculated the dose response to calmodulin at a constant calcium concentration of $[Ca^{2+}]$ = 10 μM with and without Ng. When present, the concentration of Ng was set to 20 μM [34].

Fig 2 shows the maximum amounts of each individual Ca^{2+}/CaM species relative to total CaM available for a range of [CaM]s. We observe that without Ng, we consistently have more $1Ca^{2+}/CaM$ than in the presence of Ng (Fig 2A, 2B and 2E top panels). This is easily understandable: Ng limits the availability of free calmodulin, and in its absence, we have more CaM available to bind calcium. On the other hand, when we look at CaM species that have multiple calcium ions bound to them, we see a crossover of the 2 curves as the total [CaM] increases. This is particularly striking for $3Ca^{2+}/CaM$ and $4Ca^{2+}/CaM$ (Fig 2C, 2D and 2E bottom panels). For these species, limiting the available free CaM can be beneficial since this increases the ratio $[Ca^{2+}]$:$[CaM]_{free}$, resulting in higher number of calmodulin proteins bound to multiple calcium ions. Fig 2E shows the dose response in the physiological range of CaM concentration.

While the calculated effects may seem small, they are amplified by the fact that these multi-calcium-bound calmodulin species have a higher CaMKII binding rate, and render the bound CaMKII more susceptible to phosphorylation (Table 1). These observations lead to an interesting question: is the higher relative concentration of $4Ca^{2+}/CaM$ resulting truly from the competition between calcium and Ng for CaM or does CaMKII play a role as a leaky buffer for different multi-calcium-bound forms? To answer this question, we repeated the simulations in the absence of any CaMKII. In this case, we observed an even more pronounced effect of Ng in the increase of multi-calcium-bound states of CaM for certain CaM concentrations (S1 Fig) but the overall trend remains the same as in the presence of CaMKII (Fig 2). Thus, we conclude that the relative distribution of different calcium-bound forms of CaM are indeed a result of competition between Ng and Ca^{2+} for CaM.

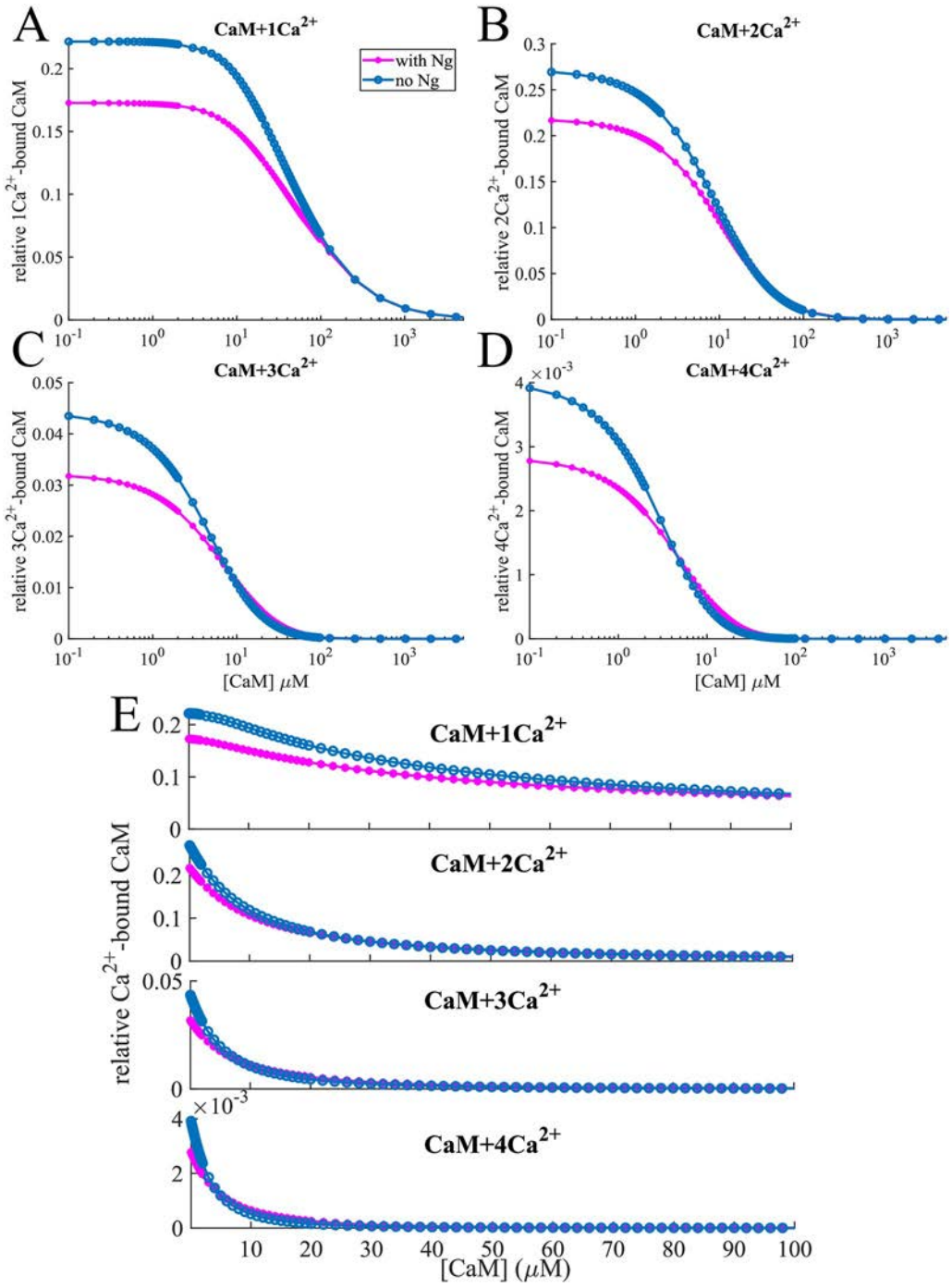

Fig 2. CaM binding calcium. Relative concentration of (A) 1-, (B) 2-, (C) 3- and (D) 4-calcium-bound calmodulin vs. total [CaM] at constant $[Ca^{2+}]$ = 10 μM. For most of the calcium-bound forms, the relative concentration is lower in the presence of neurogranin. However, in the case of 3- and 4-calcium-bound calmodulin the situation is reversed for certain [CaM]: Ng competes with Ca^{2+} for free calmodulin, which allows a regime where the concentration of these "multi-calcium-bound" forms is higher. As the concentration of calmodulin is further increased, the $[Ca^{2+}]$:[*CaM*] ratio decreases and these forms die out. Thus at high [CaM] the effects of Ng are diminished. (E) shows the same effect for physiologically relevant [CaM].

https://doi.org/10.1371/journal.pcbi.1008015.g002

mCaMKII phosphorylation dose response curve depends nonmonotonically on Ng

Next we looked at the effect of presence or absence of Ng on the phosphorylation of mCaMKII at different [*CaM*]. When we look at phosphorylated mCaMKII (p-mCaMKII) bound to different species of calmodulin, we see that Ng has very different effects on these different species (Fig 3). Phosphorylation by 1- and 2- Ca^{2+}/CaM in the presence of Ng is lower than that in the absence of Ng for $[CaM] \approx 1 - 100$ μM (Fig 3A, 3B and 3E top 2 panels). As [CaM] increases, the presence of Ng becomes less relevant and the 2 curves converge. The situation is quite different for 3- and more importantly 4- Ca^{2+}/CaM species (Fig 3C, 3D and 3E bottom 2 panels). At slightly higher [CaM], the competition with Ng for free CaM plays an important role: a higher proportion of the CaM molecules have 4 calcium ions bound to them in the presence of Ng than in the absence as discussed above, and these CaM molecules give a much higher phosphorylation rate to the CaMKII monomers that they bind. However, these species only exist at relatively lower [CaM]s—as [CaM] increases, the ratio $[Ca^{2+}]:[CaM]_{free}$ decreases, the effect of Ng becomes insubstantial since the 1- and 2- Ca^{2+}/CaM species are responsible for mCaMKII phosphorylation at these concentrations. The dose response curves in the physiologically relevant range of [CaM] ($\sim 10 - 50$ μM, [57–59], Fig 3E) show that the influence of Ng on mCaMKII phosphorylation is most prominent in this range.

The dose response of total mCaMKII phosphorylation to CaM is shown in Fig 4A. Here, the count of p-mCaMKII includes the molecules that have released the Ca^{2+}/CaM complexes they were bound to while being phosphorylated. Thus, this count is higher than the total sum of the p-mCaMKII molecules bound to different species of Ca^{2+}/CaM plotted in Fig 3. With this information, we can interpret the results shown in Fig 4A after having examined those in Fig 3. Here, the first local maximum is caused by phosphorylation of mCaMKII bound to 4 – Ca^{2+}/CaM. Since there are more of these species in the presence of Ng (Fig 3D), this peak is more prominent when Ng is present in the system. The second peak is caused by phosphorylation of the mCaMKII bound to 1- and 2- Ca^{2+}/CaM. Finally, at ultra-high [CaM] calcium-free CaM becomes the relevant species, which can still bind CaMKII, albeit with a low affinity (Table 1). Since these species do not allow the phosphorylation of the bound mCaMKII the phosphorylation levels reach 0 at ultra-high [CaM]. These species play an important role at higher [CaM], where the role of Ng is less important. Therefore, total p-mCaMKII increasingly overlaps as [CaM] is increased irrespective of the presence or absence of Ng. The implications of this result can be understood by comparing Fig 4B and 4C, which show the dynamics of mCaMKII phosphorylation with and without Ng at two distinct [CaM]s, an average (30 μM) and an upper bound to physiological (100 μM). The effect of Ng is reversed in the case of these two CaM concentrations: when $[CaM] = 30$ μM, Ng increases mCaMKII phosphorylation level, and when $[CaM] = 100$ μM Ng decreases the overall phosphorylation of CaMKII.

Thus, Ng affects the dose response of mCaMKII phosphorylation to CaM in a nonmonotonic manner and these effects can be clearly understood by examining the effect of this scaffolding molecule on Ca^{2+}/CaM species and their ability to activate mCaMKII.

Ng modulates mCaMKII phosphorylation in response to a Ca^{2+} spike

In dendritic spines, the steady state calcium concentration is $\sim 100nM$ [60]. Any Ca^{2+} influx is rapidly buffered in the spine, so that $[Ca^{2+}]_{free}$ falls back to near steady state levels within $\sim$ 100 ms [61]. To better mimic the experiments, we next used dynamic Ca^{2+} inputs. These inputs were designed such that the free Ca^{2+} ions in the spines reach ~ 10 μM at the peak of the signal and fall back to near steady state levels within ∼100 ms [61–66]. We note that this Ca^{2+} is not representative of the actual amount of calcium ions entering the spine, but rather

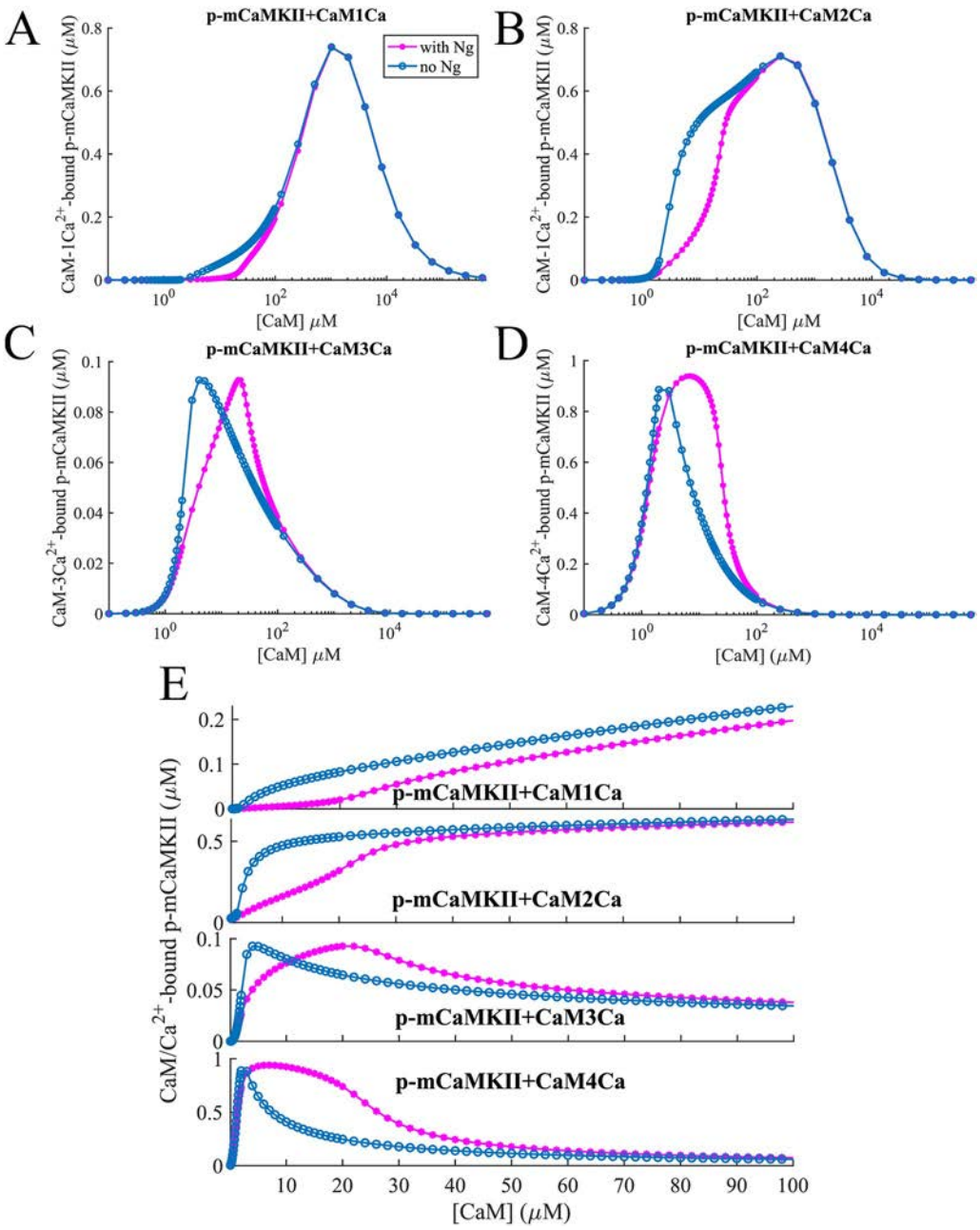

Fig 3. mCaMKII phosphorylation. Dose response of phosphorylated mCaMKII molecules bound to (A) 1-, (B) 2-, (C) 3- and (D) 4-calcium states of CaM-Ca^{2+} as shown in Fig 2. At low [CaM], the "multi-calcium-bound" forms of calmodulin play an important role. This is amplified by the fact that these forms when bound to CaMKII give it higher phosphorylation rates (Table 1). (E) sows the same effect for physiologically relevant [CaM]. In these simulations, input $[Ca^{2+}]$ = 10 μM constant.

https://doi.org/10.1371/journal.pcbi.1008015.g003

represents Ca^{2+}_{free}. This is because our model does not include any explicit calcium buffers and only simulates calcium buffering mathematically.

Before simulating the calcium spike, we allow the system to equilibrate. There is some basal level of mCaMKII phosphorylation even at the low calcium concentrations (∼ 100 nM) observed in the spine in equilibrium. To achieve a given $[Ca^{2+}]_{free}$ in different conditions, the

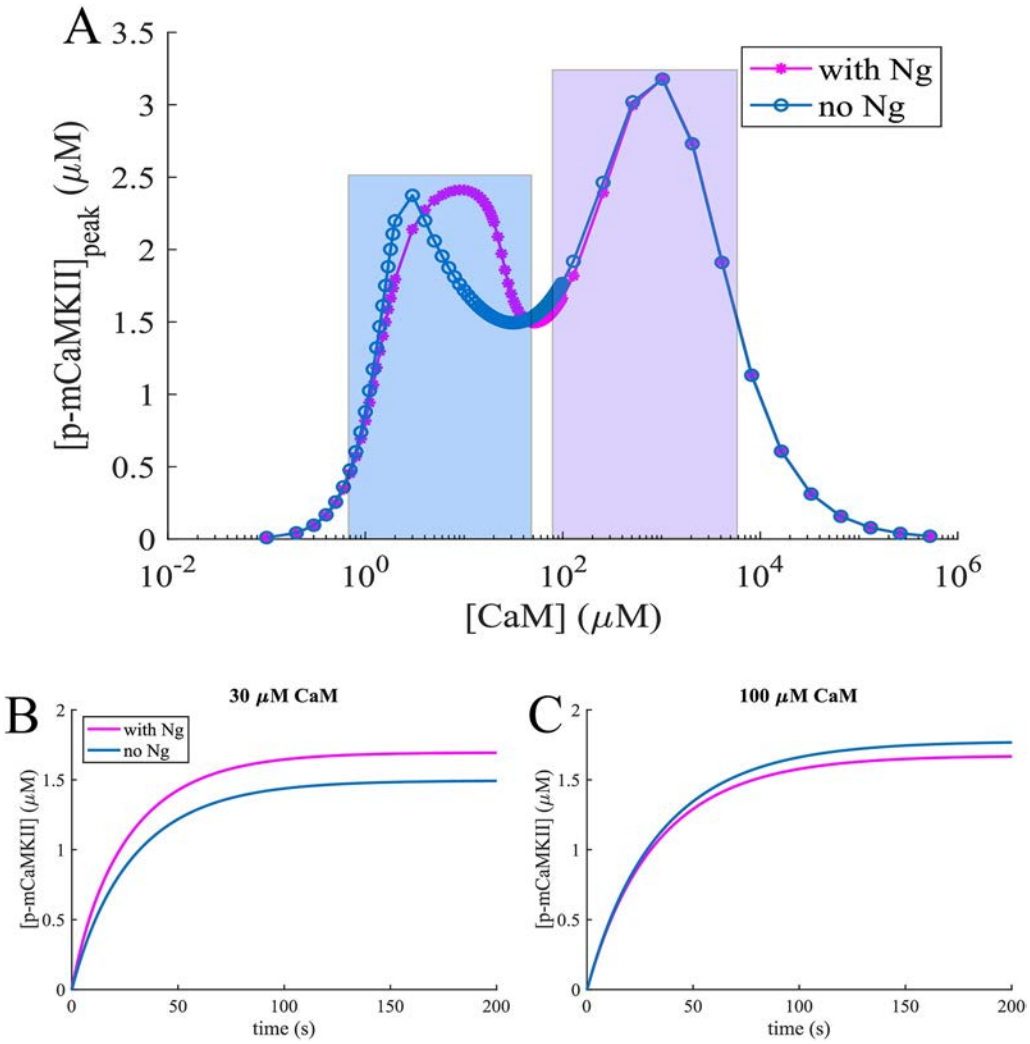

Fig 4. Phosphorylation dynamics of CaMKII monomers. mCaMKII phosphorylation dependence on [CaM] and Ng. (A) Steady state phosphorylated mCaMKII concentration as a function of total CaM concentration in the presence of 10 μM Ca^{2+} with (pink lines) and without (blue lines) Ng. The first peak (highlighted in blue rectangle) is caused by CaM molecules bound to 3-4 Ca^{2+} ions, while the second peak is caused (violet rectangle) by CaM molecules bound to 1-2 Ca^{2+}s. (B) and (C) Dynamics of mCaMKII (80 μM) autophosphorylation and dephosphorylation by PP1, in the presence of constant $[Ca^{2+}]$ = 10 μM with and without Ng, with $[CaM]$ = 30 μM and $[CaM]$ = 100 μM respectively.

https://doi.org/10.1371/journal.pcbi.1008015.g004

concentration of total calcium varies depending on the conditions simulated, and so does the basal mCaMKII phosphorylation level (S2 Fig). To enable direct comparison, we look at the difference of the peak and basal phosphorylation for each condition, as well as the Area Under the Curve (AUC), peak time, and the decay time of phosphorylation levels.

We first investigated the dependence of maximum mCaMKII phosphorylation on the amplitude of the $[Ca^{2+}]_{free}$ pulse. In Fig 5, the horizontal axis represents the "measured" $[Ca^{2+}]_{free}$ and the vertical axis shows the level of maximal mCaMKII phosphorylation. We note that for any $[Ca^{2+}]_{free}$ the response is higher in the absence of Ng, indicating that even for very small $[Ca^{2+}]$ spikes, the availability of CaM is the limiting factor for mCaMKII phosphorylation. This is further confirmed by the fact that as the size of the Ca^{2+} spike increases, the maximum mCaMKII phosphorylation levels in the presence and absence of Ng diverge from each other as they reach saturation. This observation is true for p-mCaMKII bound to any

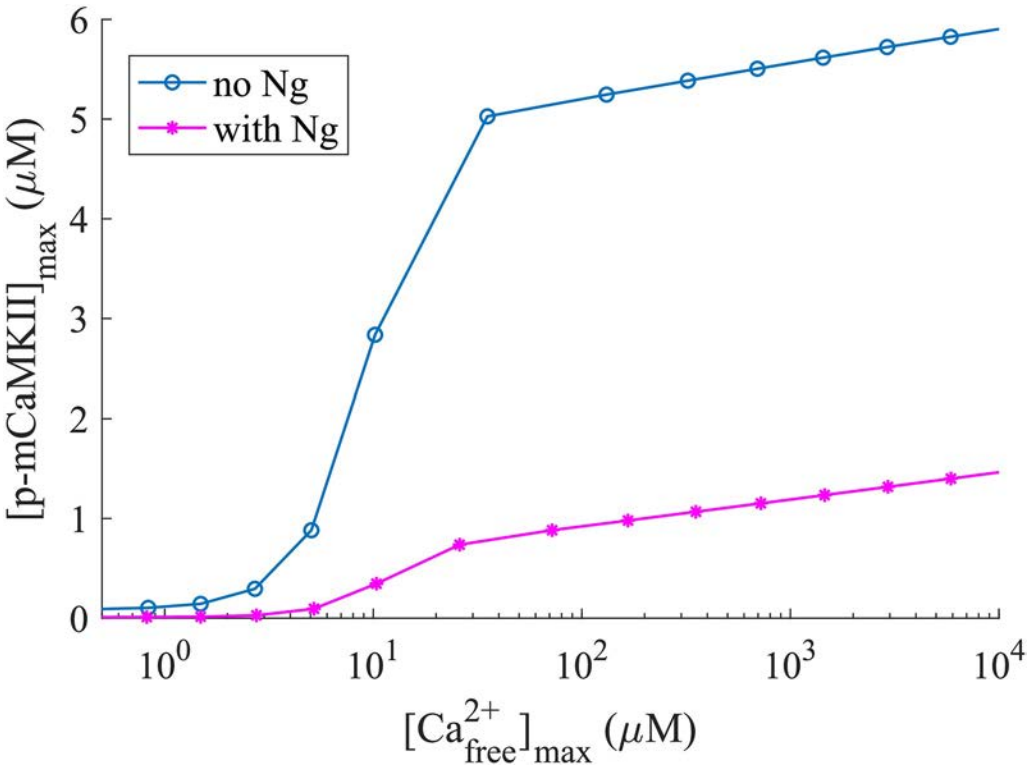

Fig 5. Maximum phosphorylated monomeric CaMKII concentration for different concentrations of Ca^{2+} spikes with [CaM] = 30 μM. The horizontal axis represents the free calcium available at the peak of the spike.

https://doi.org/10.1371/journal.pcbi.1008015.g005

species of Ca^{2+}/CaM, and, as expected, with increasing amplitude of Ca^{2+} spikes, the largest role is played by CaMs that are bound to 4 Ca^{2+}s (S3 Fig). This observation, counter-intuitive as it might seem, highlights the importance of the temporal dynamics of the reactions, and demonstrates that drawing conclusions about the system based solely on steady-state considerations alone can be misleading.

The dynamics of mCaMKII phosphorylation is shown in Fig 6A for a range of physiological CaM concentrations including the upper limit of 100 μM. As we can see, even in this extreme case Ng decreases mCaMKII phosphorylation, indicating that [CaM] is the limiting factor. Interestingly, the phosphorylation dynamics with Ng and at 50 μM [CaM] are identical to those without Ng at 30 μM [CaM]. This similarity can be easily understood by looking at the concentrations of Ng-bound CaM (CaM.Ng) at different [CaM]s. As shown in the inset of Fig 6A, when $[CaM] = 10\ \mu M$ nearly all of it is bound to Ng, and when $[CaM] > 20\ \mu M$ approximately 20 μM of it is bound to Ng.

Further comparing the total amount of mCaMKII phosphorylation over time (Area Under the Curve or AUC) as well as the relative peak phosphorylation levels (Fig 7A and 7C), we see that the presence of Ng makes a striking difference—Ng dramatically impairs phosphorylation of mCaMKII. However, at extreme high [CaM] (100 μM), the system is robust to the presence of Ng although the latter still modulates the level of phosphorylation. The presence of Ng does not appear to have a dramatic effect on the peak time or phosphorylation lifetime, which we define as the time it takes to attain 10% of the peak phosphorylation level (Fig 7E and 7G). This is expected; once phosphorylated, the mCaMKII molecules can be dephosphorylated by PP1, which works independently of Ng and of any other molecule in our model.

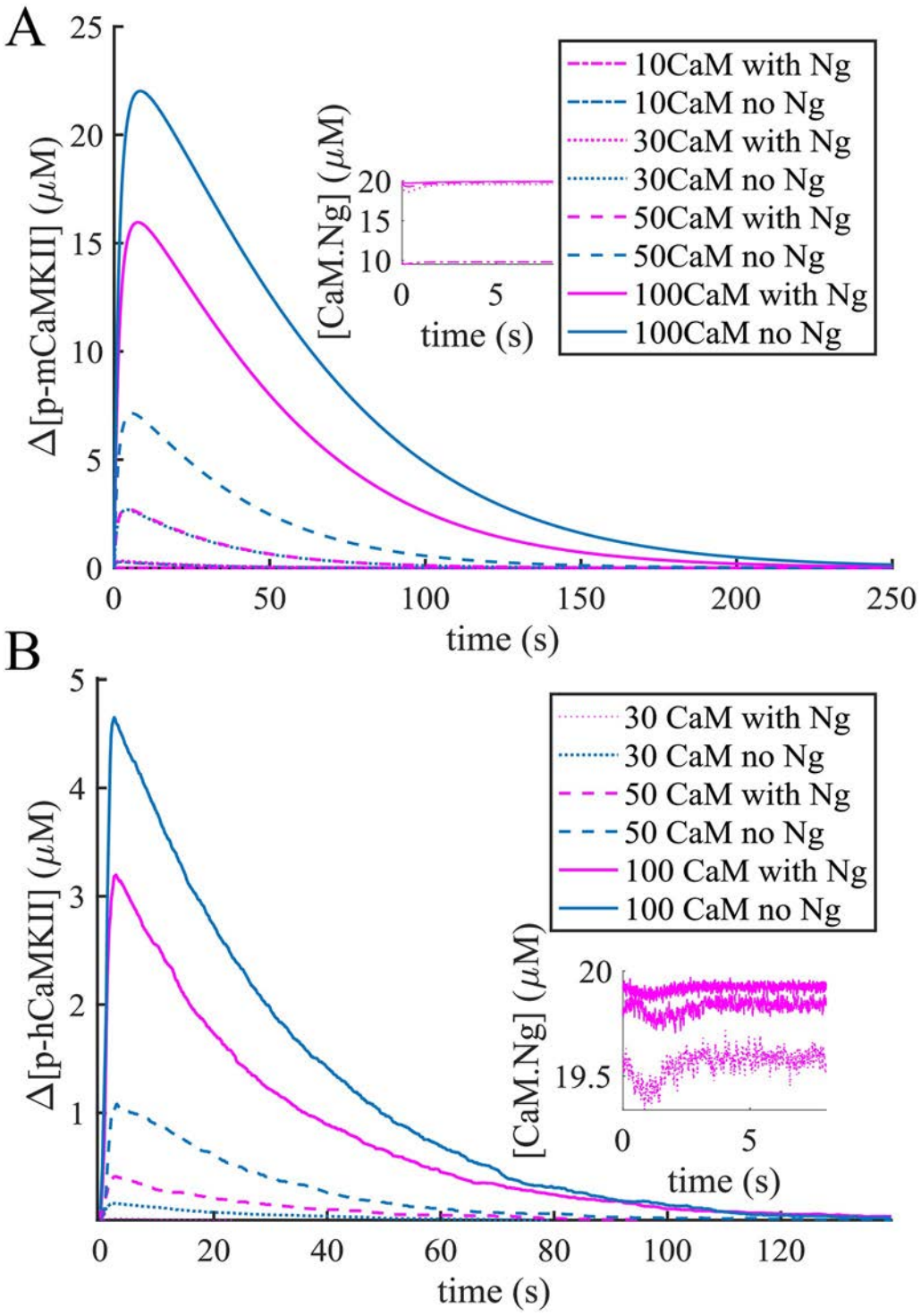

Fig 6. CaMKII phosphorylation in response to a calcium spike. The rise in CaMKII phosphorylation level as a response to a $[Ca^{2+}]_{free}$ = 10 μM spike with monomers (A) and holoenzymes (B) for different conditions. The response of the holoenzyme at [CaM] = 10 μM was not significant and is not shown here. The instets show that when $[CaM] > 20$ μM, nearly 20 μM of it is bound to Ng.

https://doi.org/10.1371/journal.pcbi.1008015.g006

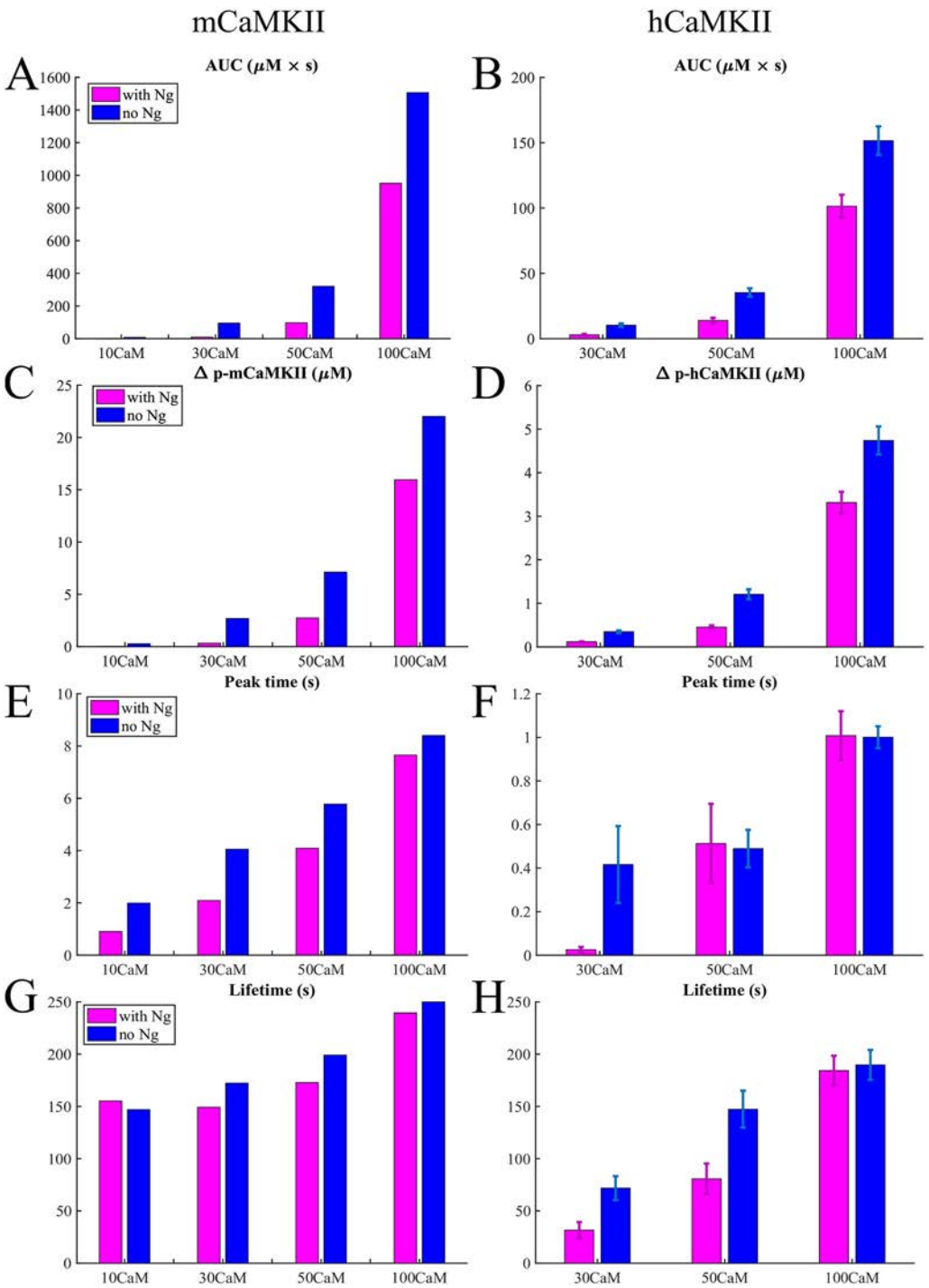

Fig 7. Quantifying the response to a calcium spike. Bar graphs in different conditions for the monomers and holoenzymes respectively of Area Under the Curve (AUC) (A) and (B), the maximum increase in phosphorylated CaMKII concentration (C) and (D), the time of the phosphorylation level reaching its peak (E) and (F), and the lifetime defined in the main text (G) and (H) in response to a 10 μM Ca^{2+} pulse.

https://doi.org/10.1371/journal.pcbi.1008015.g007

We note that our simulations result in a phosphorylation lifetime on the order of minutes. This is longer than the time constants of 6 and 45 seconds measured in Ref. [42]. This discrepancy may be because the dephosphorylation time constants measured in spines might be a result of the spatial organization of the spine, not taken into account here, or additional molecular pathways that are not part of the current model.

CaMKII holoenzyme phosphorylation is robust against fluctuations of $[Ca^{2+}]_{free}$

We next investigated the role of Ng in governing the phosphorylation dynamics of the CaMKII holoenzyme (hCaMKII) using a stochastic agent-based approach. The details of the model development for hCaMKII are given in the Methods. Briefly, the initial conditions of Model 2 contain only CaMKII holoenzymes in the simulated PSD volume $V = 0.0156\ \mu m^3$ volume, and the model does not contain any reactions that would allow disintegration of or subunit exchange between holoenzymes. From here onwards, when we refer to CaMKII phosphorylation in the holoenzyme, we are referring to subunits within the holoenzyme that are phosphorylated and we represent this using hCaMKII phosphorylation.

Fig 6B shows the average hCaMKII phosphorylation in response to a ∼10 μM single Ca^{2+} spike for $[CaM] = 30\ \mu M$, $50\ \mu M$, and $100\ \mu M$, respectively. We also conducted simulations at $[CaM] = 10\ \mu M$; however at this CaM concentration, hCaMKII did not react to 10 μM Ca^{2+} pulses. The results shown are an average of ∼30 runs of the stochastic model. In the simulations with $[CaM] = 30\ \mu M$, the mean peak and standard deviation of $[Ca^{2+}]_{free}$ were 10.7 ± 1.6 μM in the case with no Ng and 10.3 ± 1.2 μM in the case with Ng.

We note that $[CaM]$ = 30 μM corresponds to 283 CaM molecules in our stochastic model. Only a fraction of these molecules binds calcium during the calcium transient, and only a fraction of these complexes bind a hCaMKII subunit. Furthermore, only a fraction of these hCaMKII subunits have an active neighbor that can phsophorylate them. Thus, hCaMKII would not always react to the 10 μM free calcium spike, and sometimes there will be no detected phosphorylated hCaMKII subunits. The events with no detected hCaMKII phosphorylation were not taken into account in the calculations shown in Figs 6B and 7B, 7D, 7F and 7H. In the absence of Ng, 36 out 60 simulations yielded a change in phosphorylation levels. In the presence of Ng, we had to conduct 120 simulations to get 31 simulations that resulted in noticeable hCaMKII phosphorylation. From these observations, we conclude that the probability of hCaMKII phosphorylation is affected by the presence of Ng.

When $[CaM] = 50\ \mu M$, the mean peak and standard deviation of $[Ca^{2+}]_{free}$ were 9.4 ± 1.2 μM in the case with no Ng and 10.2 ± 1.3 μM in the case with Ng. Finally, in the extreme case when $[CaM] = 100\ \mu M$ the corresponding numbers were 9.2 ± 1.3 μM both with and without Ng. In the inset of Fig 6B we show again that when $[CaM] > 20\ \mu M$ nearly 20 μM of it is bound to Ng. In this light, it might be surprising that the response curves for [CaM] = 30, and 50 μM do not overlap as nicely as they do in Fig 6A. This is because the individual simulations are stochastic; comparing the results in Fig 7B, 7D, 7F and 7H we can see that the average results of 30 simulations for [CaM] = 30 μM without Ng, and [CaM] = 50 μM with Ng are consistent with each other within the error bars presented.

By comparing the Figs 6A, 6B and 7A, 7C, 7E and Fig 7B, 7D and 7F, we notice that with the same amount of CaM present in the simulation, the holoenzyme reacts significantly faster to the calcium signal (see the peak time) than the monomeric CaMKII but the phosphorylation level is also much lower. This is understandable: while in the case of monomers any active molecule of CaMKII can bind and phosphorylate another, provided the latter is bound to Ca^{2+}/CaM, in the case of the holoenzyme a given subunit can only be phosphorylated by one (and only

one) of its neighbors. Since the phosphorylation of a given subunit in the holoenzyme is still dependent on it being bound to a $[Ca^{2+}/CaM]$ complex, this condition becomes harder to satisfy shortly after the $[Ca^{2+}]$ drops back to $\sim$100nM. And with the holoenzyme the cessation of phosphorylation happens more rapidly, since the conditions imposed for phosphorylation of a given subunit are more rigid. Thus, these more rigid conditions explain both the lower phosphorylation level, and the shorter timescales exhibited by the holoenzyme.

This result tells us that the holoenzyme is more robust to Ca^{2+} fluctuations than the monomers. When the holoenzyme does react to a calcium signal, the phosphorylation lifetime is comparable to that of the monomers (Fig 7G and 7H). And as in the case for monomers, the presence of Ng modulates the effect of the calcium signal at physiological calmodulin concentrations.

A leaky integrator of $[Ca^{2+}]$ signals

Having established the dynamics of mCaMKII and hCaMKII phosphorylation for a single spike of Ca^{2+}, we next investigated the response of hCaMKII to multiple Ca^{2+} spikes. The multiple spikes were designed to mimic experimental stimuli of a train of Ca^{2+} spikes [42, 67–69]. Fig 8 shows the average response of hCaMKII phosphorylation to 10 calcium pulses at 0.5 Hz. As we can see, even with 10 Ca^{2+} pulses in the case of $[CaM] = 30\ \mu M$, the hCaMKII phosphorylation is very small, particularly in the presence of Ng. In fact, even with 10 calcium pulses, only 25 out of 30 simulations resulted in a non-negligible difference of hCaMKII phosphorylation levels in the presence of Ng, and only 28 out of 30 in the absence of Ng. Therefore, multiple spikes increase and even out the probability of hCaMKII phosphorylation but not the overall phosphorylation level in the presence or absence of Ng.

As before, the presence of Ng makes less difference when [CaM] is higher (100 μM), and this system is far more sensitive to calcium signals (Fig 8A, 8C and 8D).

To compare the effect of multiple Ca^{2+} pulses versus a single pulse, we calculated the ratios of the hCaMKII phosphorylation metrics, AUC and maximum change in phosphorylation for 10 to 1 calcium pulses. This ratios are shown in Fig 8B for all 6 conditions tested. As can be seen here, for average physiological conditions, a 10-fold increase in Ca^{2+} signal results in a more modest increase in hCaMKII phosphorylation. With the exception of 100 μM (ultrahigh) CaM concentration, the ratio of the changes in phosphorylated hCaMKII concentrations is consistently lower than 10, and even the ratios of AUCs approach 10 only for [CaM] = 50 μM in the absence of Ng. This result indicates a leakage in the process of the calcium signal integration through hCaMKII phosphorylation. To further investigate the leakiness of hCaMKII phosphorylation, we calculated hCaMKII phosphorylation in response to 30 Ca^{2+} pulses (Fig 9) at average physiological [CaM]. From Fig 9A, we observe that the rate of increase in phosphorylation level decreases as more calcium pulses are added. This leakage of the calcium signal integration is caused by dephosphorylation of hCaMKII by PP1 and has recently been observed experimentally *in vivo* [69].

Since these simulations are conducted stochastically, the timing of Ca^{2+} signals is also stochastic, and not exactly synchronized across the multiple runs. Fig 9B shows hCaMKII phosphorylation in response to a train of 0.5 Hz Ca^{2+} pulses for 3 individual runs. We see that the phosphorylation level rises in a stepwise manner in response to each calcium spike.

To better characterize hCaMKII as a leaky integrator and the effect of Ng, we fit the hCaMKII phosphorylation curves at a physiological $[CaM] = 30\ \mu M$ to the leaky integrator equation $x = k - k \cdot e^{-a \cdot t}$, where k is the maximum possible change of phosphorylation level and a is the overall phosphorylation rate (Fig 7C). The curve fitting tool from *MATLAB* was used for this purpose. The response with Ng was characterized by the equation $0.36 - 0.36 \cdot e^{-0.045 \cdot t}$ with an

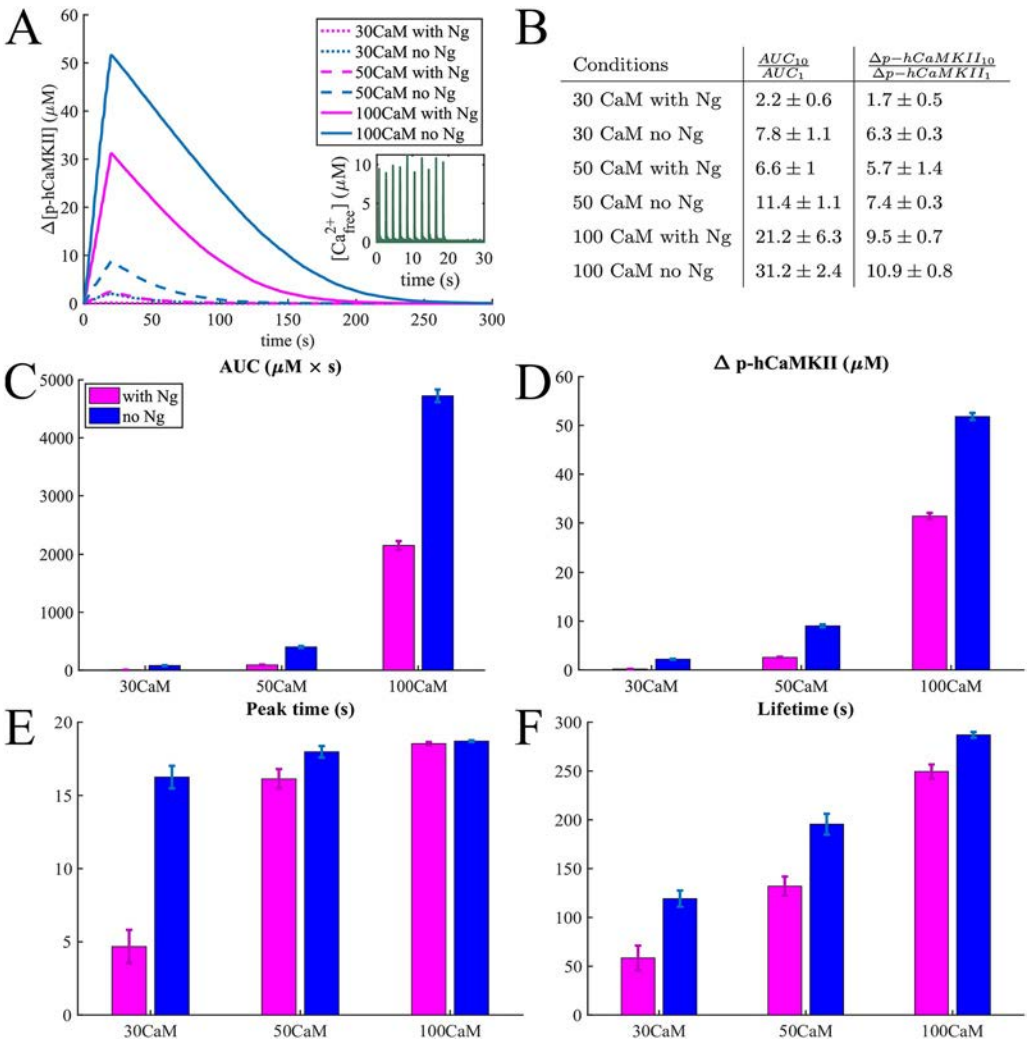

Conditions	$\frac{AUC_{10}}{AUC_1}$	$\frac{\Delta p-hCaMKII_{10}}{\Delta p-hCaMKII_1}$
30 CaM with Ng	2.2 ± 0.6	1.7 ± 0.5
30 CaM no Ng	7.8 ± 1.1	6.3 ± 0.3
50 CaM with Ng	6.6 ± 1	5.7 ± 1.4
50 CaM no Ng	11.4 ± 1.1	7.4 ± 0.3
100 CaM with Ng	21.2 ± 6.3	9.5 ± 0.7
100 CaM no Ng	31.2 ± 2.4	10.9 ± 0.8

Fig 8. Responses to trains of 10 Ca^{2+} pulses. (A) An average phosphorylation of CaMKII holoenzyme in response to 10 Ca^{2+} pulses at 0.5 Hz averaged over 30 simulations with 63 holoenzymes and 30 μM 50 μM, and 100 μM calmodulin. (B) Table of the ratios of the Area under the curve and maximum change in phosphorylation level in response to 10 and 1 Ca^{2+} pulses in different conditions. Bar graphs comparing the (C) Area Under the Curve (AUC), (D) the maximum increase in the hCaMKII phosphorylation concentration, (E) the time of the phosphorylation level reaching its peak, and (F) the lifetime defined in the main text in response these Ca^{2+} pulses.

https://doi.org/10.1371/journal.pcbi.1008015.g008

$R^2 = 0.9683$ and the response without Ng by $7.24 - 7.24 \cdot e^{-0.025 \cdot t}$ with an $R^2 = 0.9979$. This result demonstrates that Ng not only regulates the leak rate of the integrator, but also severely reduces the maximum possible phosphorylation level. The results in Figs 8 and 9 predict that hCaMKII phosphorylation behaves as a leaky integrator of calcium signals, and that the presence of Ng dramatically affects the properties of this integrator.

We also found that hCaMKII activation through Ca^{2+}/CaM binding does not integrate over calcium signals in the same way hCaMKII phosphorylation does. Fig 10 shows 3 representative examples of the changes of CaM-bound hCaMKII concentration in response to Ca^{2+} spikes at $CaM = 50$ μM and in the presence and absence of Ng. This finding is consistent with recent observations in [44]. We observe that when Ng is present (Fig 10A) hCaMKII activation through CaM binding reaches about the same level at every Ca^{2+} spike. This is what was observed experimentally by [44]. On the other hand, the subsequent decrease of CaM-bound-

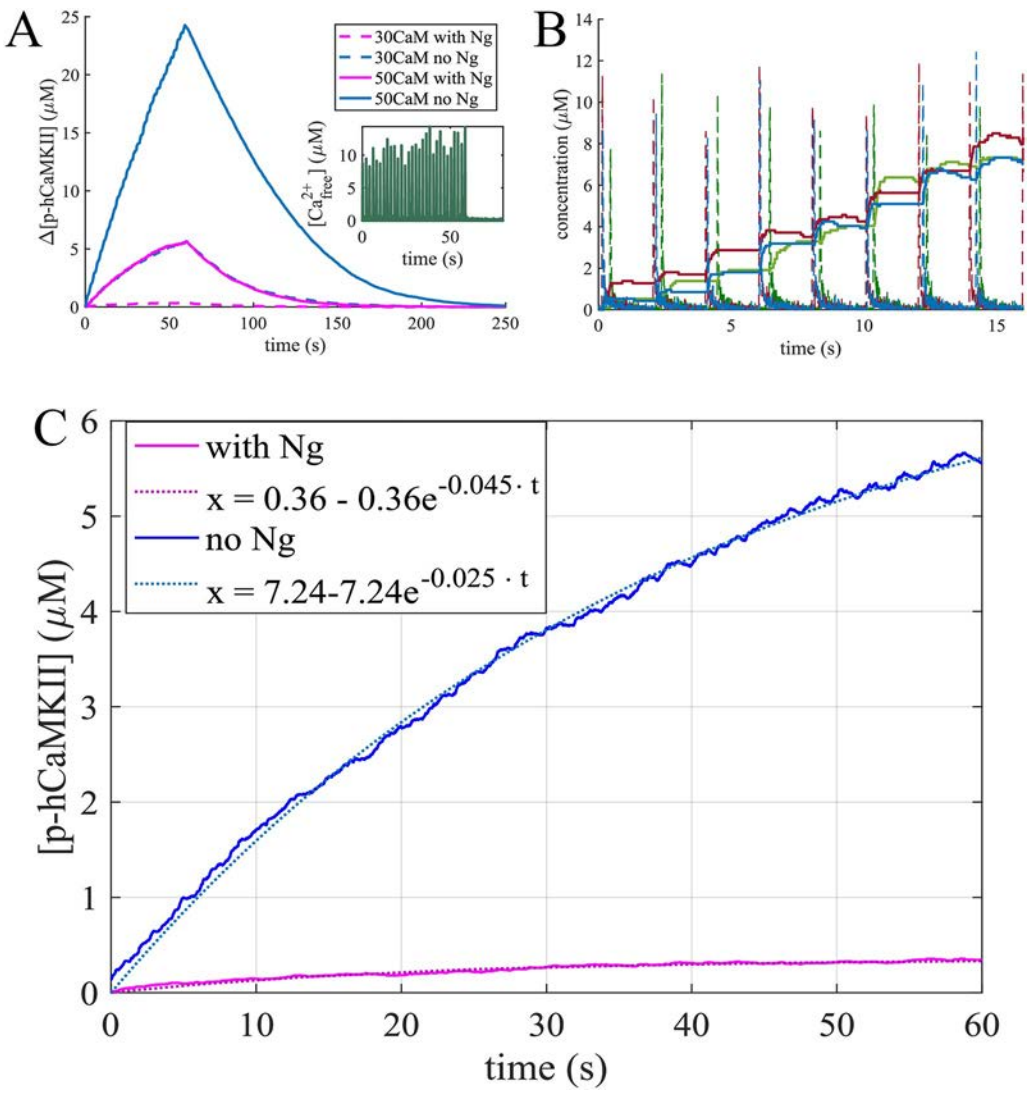

Fig 9. Responses to trains of 30 Ca^{2+} pulses. (A) An average phosphorylation of CaMKII holoenzyme in response to 30 Ca^{2+} pulses at 0.5 Hz averaged over 30 simulations with 63 holoenzymes and 30 μM, and 50 μM calmodulin. (B) Three individual simulations: the response of hCaMKII phosphorylation level (solid lines) change to the calcium spikes (dashed lines). (C) Fitting the leaky integrator. The average response to 30 Ca^{2+} pulses was fitted to a curve of the form $x = k - k \cdot e^{-a \cdot t}$ with and without Ng and $[CaM]$ = 30 μM, with the curve fitting tool from MATLAB. The parameters obtained are: k = 7.24, a = 0.025 with an R^2 = 0.9979 without Ng and k = 0.36, a = 0.045 with an R^2 = 0.9683 with Ng. Thus Ng not only changes the leaking rate of the integrator, but significantly lowers the maximum possible phosphorylation level.

https://doi.org/10.1371/journal.pcbi.1008015.g009

hCaMKII after each pulse stops at higher concentrations after later Ca^{2+} spikes. This is particularly evident in the absence of Ng (Fig 10B). In fact, in this case, we can also see a slight increase in peak levels of CaM-bound hCaMKII. When we look at only unphosphorylated hCaMKII molecules (u-hCaMKII) bound to CaM, however, we see that the peaks of these curves slightly decrease, while the troughs remain at the same level (S4A and S4B Fig). This prediction was also observed experimentally with T286A CaMKII mutation which make CaMKII unable to be phosphorylated [44]. Finally, when we look at the average peak concentration of CaM bound hCaMKII and u-hCaMKII corresponding to each Ca^{2+} pulse over 30 trials we see that on average peaks corresponding to later pulses are slightly higher for CaM/hCaMKII and slightly lower for CaM/u-hCaMKII species (S4C and S4D Fig). It is noteworthy that, while

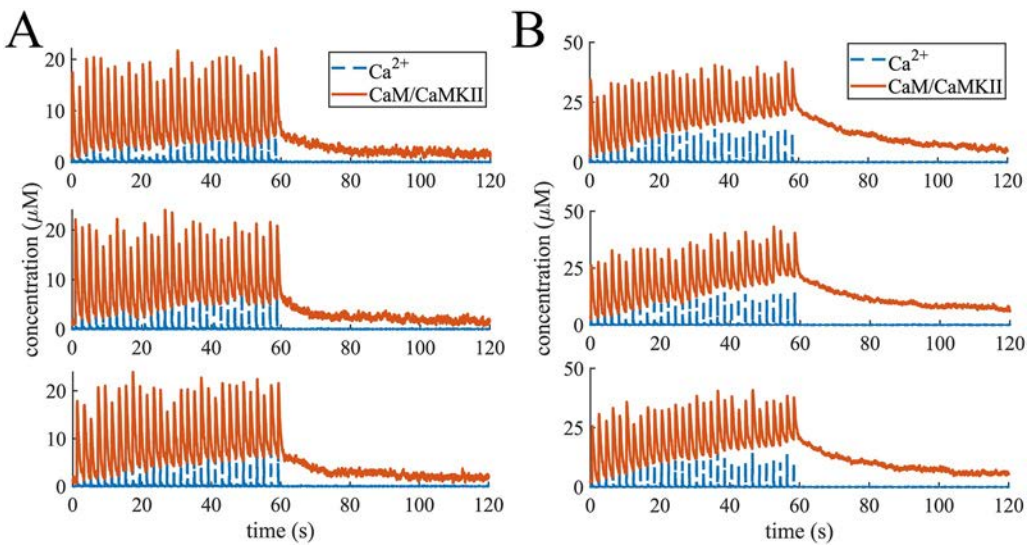

Fig 10. Responses to trains of 30 Ca^{2+} pulses. 3 representative curves of CaMKII subunits in the holoenzyme binding CaM in response to Ca^{2+} spikes at [*CaM*] = 50 μM with (A) and without (B) Ng.

https://doi.org/10.1371/journal.pcbi.1008015.g010

Chang et al [44] observed no increase in CaM/CaMKII peak concentration with later glutamate uncaging pulses, they also found that phosphorylation at T305 site accelerate CaMKII inactivation. The fact that our model does not include this phosphorylation site, might be the reason we see an average increase in peak CaM-bound hCaMKII concentration.

Discussion

CaMKII phosphorylation is a fundamental process downstream of Ca^{2+}-influx in the PSD. There have been many studies focused on the interactions of Ca^{2+}, CaM, and CaMKII, and their role in the dynamics of CaMKII phosphorylation [7, 21, 25, 30, 39, 70, 71]. This pathway has also been the focus of computational modeling including explorations of phenomenological models pursuing possibilities of switch-like behavior [11, 33, 35, 37, 38, 40, 72, 73], as well as the effects of intraholoenzyme subunit exchanges on CaMKII activation stability [74], and the role of calmodulin-trapping in maintanance of CaMKII autophosphorylation [39].

In this work, we developed computational models to consider the interactions of both mCaMKII and hCaMKII with CaM in the presence and absence of Ng. These models were built to represent the interactions between different molecules in this pathway based on experimental data with the goal of finely dissecting the behavior of CaMKII phosphorylation. The comparison of our modeling results with the experimental results by Chang et al. [44, 69] can elucidate which aspects of the observed CaMKII behaviour can be explained solely through the interactions of the considered molecules, and which ones can't. We generate the following predictions from our model: *first*, the presence of a scaffolding molecule, Ng, has a nonmonotonic effect on the dose response curve of CaMKII phosphorylation in response to Ca^{2+} influx. *Second*, CaMKII holoenzyme is less sensitive to Ca^{2+} signals than the equivalent number of monomers because of the restrictions in phosphorylation, and is thus less susceptible to noise and fluctuations of [Ca^{2+}]. Ng further modulates CaMKII phosphorylation in response to [Ca^{2+}] spikes in the physiological range of [CaM], indicating that [CaM] is the limiting factor for CaMKII activation. It has been observed that CaM becomes a limiting factor for CaMKII activation once regulator of calmodulin signaling (RCS) is phosphorylated, making this protein another competitor to bind CaM [75, 76]. *Finally*, we predict that in the presence of PP1,

the CaMKII holoenzyme acts as a leaky integrator of calcium signals, and Ng significantly affects both the capacity and the leak rate of this integrator (Fig 9C). Based on these findings, we predict that Ng plays a crucial role in fine-tuning the postsynaptic response to Ca^{2+} signals by canceling out the noise and increasing precision in ways that were previously not known.

Our predictions are consistent with experimental data that show that Ng knockout mice exhibit a decrease in LTP induction and spatial learning [77]. Experimental results show that impairment of the binding of Ng to CaM results in lower activity of CaMKII in the dendritic spines [77, 78]. At first sight, this finding seems contradictory to what we find here: the presence of Ng decreases CaMKII activation in our simulations. To understand this apparent inconsistency we note that in our simulations, we compared the results obtained with and without Ng while keeping the overall [CaM] the same for both cases. *In vivo* however, the scaffolding protein Ng sequesters CaM into the dendritic spines, thereby increasing the overall [CaM] in the spines that can be released upon stimulation [79]. This explanation is supported by the observation that postsynaptic injection of Ca^{2+}/CaM enhances the synaptic strength in the same manner as overexpression of neurogranin in CA1 neurons [79–81]. An additional detail, not considered in the present work, is the modulation of Ng activity through protein kinase C (PKC). Ca^{2+} influx in spines activates PKC, which phosphorylates Ng. Phosphorylated Ng has diminished ability to bind CaM [79, 82], resulting in altered dynamics of CaMKII phosphorylation and further fine-tuning of the synaptic response to stimulation. Integrating the detailed pathway of PKC-Ng interaction is the focus of a future study.

Given the wealth of models for CaMKII phosphorylation dynamics in the literature, it is important to consider our results in the context of previous findings. It has been suggested by previous models that CaMKII can exhibit bistability and act as a molecular switch ([35, 37, 38]). While the idea of CaMKII bistability is an appealing explanation behind the LTP phenomenon, it has not been without controversy. For example, one experimental demonstration of CaMKII activation hysteresis was performed *in vitro* at higher than physiological $[Ca^{2+}]$ ($> 200nM$) in the presence of NMDA receptors and in a purified system [83]. To date, to the best of our knowledge there has been no *in vivo* experimental results suggesting evidence for CaMKII bistability. Furthermore, the computational models that predict bistability at physiological Ca^{2+} concentrations require a lower Michaelis-Menten constant of CaMKII dephosphorylation by PP1 (<1 μM) than measured experimentally (11 μM, Table 1). A stochastic model of CaMKII activation by Michalski showed that CaMKII does not exhibit bistability in physiological $[Ca^{2+}]$ [72] and posited that the previous reports of bistability were perhaps the result of approximations of CaMKII dynamics to overcome the combinatorial explosion of multistate, multisubunit dynamics. Since our model accounts for the subunit level phosphorylation of CaMKII at the holoenzyme level (similar to Michalski), we did not find regimes of bistability with our model. Indeed, even if we initiated the simulation with all of the hCaMKII in the model being phosphorylated, the activation decays back to basic level at physiological $[Ca^{2+}] = 100$ nM (S4 Fig).

The role of Ng in modulating the dynamics of CaMKII, particularly, the leak rate and capacity of CaMKII phosphorylation, has multiple implications in downstream processes in a spine. Phosphorylation of CaMKII activates its kinase domain, which leads to subsequent modification of the dendritic spine and the postsynaptic density [42, 84–86]. Specifically phosphorylated CaMKII unbinds from F-actin in the spine allowing reorganization of the cytoskeleton, and rebinds this newly structured F-actin after it has been dephosphorylated [16, 84, 87–90]. These interactions with the actin cytoskeleton allow for dynamic rearrangements of the actin organization within the spine, subsequently impacting its size and shape [91–93] (Fig 11). CaMKII activation also leads to increased trafficking [94, 95] and trapping [96] of AMPA receptors at the PSD as well as an increase in the conductance of these receptors after the

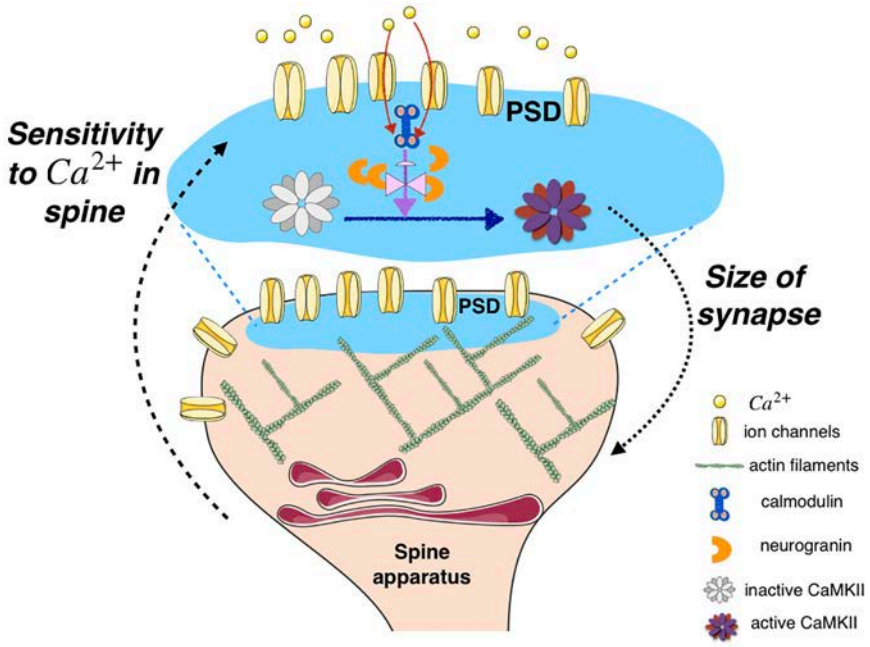

Fig 11. Schematic representation of CaMKII phosphorylation controlling sensitivity of a synapse to Ca^{2+} signals. In the PSD, influx of Ca^{2+} through the ion channel, binding of Ca^{2+} to calmodulin, and phosphorylation of CaMKII sets off the series of events associated with synaptic plasticity. In this work, we show that the competition between neurogranin sequestration of calmodulin and Ca^{2+} binding of calmodulin affects CaMKII dynamics. This has implications for the feedback between Ca^{2+} in the spine and structural plasticity of the spine, particularly size dynamics.

https://doi.org/10.1371/journal.pcbi.1008015.g011

induction of LTP [97–100]. All of these events result in changes to the size and strength of the synapse [36, 101–103] (Fig 11).

Synaptic size and strength are regulated by firing history [104] with very high precision [1]. As a synapse undergoes increased LTP, it grows larger and subsequently the Ca^{2+} transients in the spine become increasingly dilute in response to back-propagating action potentials [65]. Thus, the integration of Ca^{2+} signals is a built-in mechanism in the dendritic spine to down-regulate its sensitivity to these signals as the corresponding synapse grows larger (Fig 11). Our study shows that scaffolding molecules such as Ng can modulate these dynamics. The results of our simulations combined with experimental findings cited above point to an important role for Ng in regulating the postsynaptic response to Ca^{2+} signals. This finding adds to the growing evidence that scaffolding proteins fine-tune the signaling pathways in biological signal transduction mechanisms [105–107].

The model described here will enable the development of more detailed models of signaling events in the PSD including coupling between CaMKII, PKC, and PKA [74, 82, 108, 109], spatial organization of calcium-CaM-CaMKII dynamics building on [1, 65, 110–112], and coupling between CaMKII and actin interactions [92, 113]. Such efforts will be necessary to understand the mechanochemical coupling within spines and how they regulate information processing.

Supporting information

S1 Fig. Interaction of Ca^{2+} with CaM in the absence of CaMKII. Relative distribusion of Ca^{2+}-bound CaM species in the absence of CaMKII.
(TIF)

S2 Fig. Baseline levels of mCaMKII phosphorylation. (A) at 100 nM $[Ca^{2+}]$ different concentrations of CaM result in different baseline levels of mCaMKII phosphorylation. (B) to enable comparisons between different conditions we compare the increase in mCaMKII phosphorylation levels (Δ[p-mCaMKII]) as shown.
(TIF)

S3 Fig. Dose response to Ca^{2+} spikes. Dose response to Ca^{2+} spikes factored into p-mCaMKII bound to different species of Ca^{2+}/CaM.
(TIF)

S4 Fig. CaM-bound CaMKII. Comparing total and unphosphorylated hCaMKII (u-hCaMKII) bound to CaM with (A) and without (B) Ng: while total CaM-bound hCaMKII decays slower after a Ca^{2+} spike, CaM-bound u-hCaMKII gets down to base level immediately after the spike. C and D show the 30 peaks reached by CaM-bound hCaMKII and u-hCaMKII averaged over 30 simulations, with and without Ng respectively.
(TIF)

S5 Fig. Absence of bistability. hCaMKII does not exhibit bistability at $[Ca^{2+}] = 100nM$ in our model: even when all of hCaMKII is phosphorylated, the activation decays back to base level.
(TIF)

Acknowledgments

We thank Miriam Bell for useful discussions and assistance with making Fig 11. We thank Miriam Bell, Allen Leung and Kiersten Scott for proofreading the manuscript.

Author Contributions

Conceptualization: Mariam Ordyan, Tom Bartol, Mary Kennedy, Padmini Rangamani, Terrence Sejnowski.

Data curation: Mariam Ordyan.

Formal analysis: Mariam Ordyan.

Funding acquisition: Tom Bartol, Mary Kennedy, Padmini Rangamani, Terrence Sejnowski.

Investigation: Mariam Ordyan, Tom Bartol, Mary Kennedy, Padmini Rangamani, Terrence Sejnowski.

Methodology: Mariam Ordyan, Tom Bartol, Padmini Rangamani, Terrence Sejnowski.

Project administration: Padmini Rangamani, Terrence Sejnowski.

Software: Mariam Ordyan, Tom Bartol.

Supervision: Padmini Rangamani, Terrence Sejnowski.

Visualization: Mariam Ordyan.

Writing – original draft: Mariam Ordyan, Padmini Rangamani.

Writing – review & editing: Mariam Ordyan, Tom Bartol, Mary Kennedy, Padmini Rangamani, Terrence Sejnowski.

References

1. Bartol TM Jr, Bromer C, Kinney J, Chirillo MA, Bourne JN, Harris KM, et al. Nanoconnectomic upper bound on the variability of synaptic plasticity. Elife. 2015; 4:e10778. https://doi.org/10.7554/eLife.10778 PMID: 26618907
2. Nimchinsky EA, Yasuda R, Oertner TG, Svoboda K. The number of glutamate receptors opened by synaptic stimulation in single hippocampal spines. Journal of Neuroscience. 2004; 24(8):2054–2064. https://doi.org/10.1523/JNEUROSCI.5066-03.2004 PMID: 14985448
3. Murthy VN, Schikorski T, Stevens CF, Zhu Y. Inactivity produces increases in neurotransmitter release and synapse size. Neuron. 2001; 32(4):673–682. https://doi.org/10.1016/S0896-6273(01)00500-1 PMID: 11719207
4. Higley MJ, Sabatini BL. Calcium signaling in dendritic spines. Cold Spring Harbor perspectives in biology. 2012; 4(4):a005686. https://doi.org/10.1101/cshperspect.a005686 PMID: 22338091
5. Nevian T, Sakmann B. Spine Ca2+ signaling in spike-timing-dependent plasticity. Journal of Neuroscience. 2006; 26(43):11001–11013. https://doi.org/10.1523/JNEUROSCI.1749-06.2006 PMID: 17065442
6. Bennett MK, Erondu NE, Kennedy MB. Purification and characterization of a calmodulin-dependent protein kinase that is highly concentrated in brain. Journal of Biological Chemistry. 1983; 258 (20):12735–12744. PMID: 6313675
7. Miller SG, Kennedy MB. Regulation of brain Type II Ca2+ calmodulin-dependent protein kinase by autophosphorylation: A Ca2+-triggered molecular switch. Cell. 1986; 44(6):861–870. https://doi.org/10.1016/0092-8674(86)90008-5 PMID: 3006921
8. Rich RC, Schulman H. Substrate-directed function of calmodulin in autophosphorylation of Ca2+/calmodulin-dependent protein kinase II. Journal of Biological Chemistry. 1998; 273(43):28424–28429. https://doi.org/10.1074/jbc.273.43.28424 PMID: 9774470
9. Miller SG, Patton BL, Kennedy MB. Sequences of autophosphorylation sites in neuronal type II CaM kinase that control Ca2+-independent activity. Neuron. 1988; 1(7):593–604. https://doi.org/10.1016/0896-6273(88)90109-2 PMID: 2856100
10. Giese KP, Fedorov NB, Filipkowski RK, Silva AJ. Autophosphorylation at Thr286 of the α calcium-calmodulin kinase II in LTP and learning. Science. 1998; 279(5352):870–873. https://doi.org/10.1126/science.279.5352.870 PMID: 9452388
11. Lisman J, Schulman H, Cline H. The molecular basis of CaMKII function in synaptic and behavioural memory. Nature Reviews Neuroscience. 2002; 3(3):175. https://doi.org/10.1038/nrn753 PMID: 11994750
12. Silva AJ, Paylor R, Wehner JM, Tonegawa S. Impaired spatial learning in alpha-calcium-calmodulin kinase II mutant mice. Science. 1992; 257(5067):206–211. PMID: 1321493
13. Silva AJ, Stevens CF, Tonegawa S, Wang Y. Deficient hippocampal long-term potentiation in alpha-calcium-calmodulin kinase II mutant mice. Science. 1992; 257(5067):201–206. https://doi.org/10.1126/science.1378648 PMID: 1378648
14. Zou DJ, Cline HT. Postsynaptic calcium/calmodulin-dependent protein kinase II is required to limit elaboration of presynaptic and postsynaptic neuronal arbors. Journal of Neuroscience. 1999; 19 (20):8909–8918. https://doi.org/10.1523/JNEUROSCI.19-20-08909.1999 PMID: 10516310
15. Wu GY, Cline HT. Stabilization of dendritic arbor structure in vivo by CaMKII. Science. 1998; 279 (5348):222–226. https://doi.org/10.1126/science.279.5348.222 PMID: 9422694
16. Shen K, Teruel MN, Subramanian K, Meyer T. CaMKIIβ functions as an F-actin targeting module that localizes CaMKIIα/β heterooligomers to dendritic spines. Neuron. 1998; 21(3):593–606. https://doi.org/10.1016/S0896-6273(00)80569-3 PMID: 9768845
17. Borovac J, Bosch M, Okamoto K. Regulation of actin dynamics during structural plasticity of dendritic spines: Signaling messengers and actin-binding proteins. Molecular and Cellular Neuroscience. 2018. https://doi.org/10.1016/j.mcn.2018.07.001 PMID: 30004015
18. Okamoto KI, Narayanan R, Lee SH, Murata K, Hayashi Y. The role of CaMKII as an F-actin-bundling protein crucial for maintenance of dendritic spine structure. Proceedings of the National Academy of Sciences. 2007; 104(15):6418–6423. https://doi.org/10.1073/pnas.0701656104
19. Xia Z, Storm DR. The role of calmodulin as a signal integrator for synaptic plasticity. Nature Reviews Neuroscience. 2005; 6(4):267. https://doi.org/10.1038/nrn1647 PMID: 15803158
20. Finn BE, Forsén S. The evolving model of calmodulin structure, function and activation. Structure. 1995; 3(1):7–11. https://doi.org/10.1016/S0969-2126(01)00130-7 PMID: 7743133
21. Shifman JM, Choi MH, Mihalas S, Mayo SL, Kennedy MB. Ca2+/calmodulin-dependent protein kinase II (CaMKII) is activated by calmodulin with two bound calciums. Proceedings of the National Academy of Sciences. 2006; 103(38):13968–13973. https://doi.org/10.1073/pnas.0606433103

22. Hoffman L, Chandrasekar A, Wang X, Putkey JA, Waxham MN. Neurogranin alters the structure and calcium-binding properties of calmodulin. Journal of Biological Chemistry. 2014; p. jbc–M114. https://doi.org/10.1074/jbc.M114.560656

23. Chao LH, Stratton MM, Lee IH, Rosenberg OS, Levitz J, Mandell DJ, et al. A mechanism for tunable autoinhibition in the structure of a human Ca2+/calmodulin-dependent kinase II holoenzyme. Cell. 2011; 146(5):732–745. https://doi.org/10.1016/j.cell.2011.07.038 PMID: 21884935

24. Hanson PI, Schulman H. Inhibitory autophosphorylation of multifunctional Ca2+/calmodulin-dependent protein kinase analyzed by site-directed mutagenesis. Journal of Biological Chemistry. 1992; 267 (24):17216–17224. PMID: 1324926

25. Patton BL, Miller SG, Kennedy MB. Activation of type II calcium/calmodulin-dependent protein kinase by Ca2+/calmodulin is inhibited by autophosphorylation of threonine within the calmodulin-binding domain. Journal of Biological Chemistry. 1990; 265(19):11204–11212. PMID: 2162838

26. Hanson PI, Kapiloff MS, Lou LL, Rosenfeld MG, Schulman H. Expression of a multifunctional Ca2 +/calmodulin-dependent protein kinase and mutational analysis of its autoregulation. Neuron. 1989; 3 (1):59–70. https://doi.org/10.1016/0896-6273(89)90115-3 PMID: 2619995

27. Hanson PI, Meyer T, Stryer L, Schulman H. Dual role of calmodulin in autophosphorylation of multifunctional CaM kinase may underlie decoding of calcium signals. Neuron. 1994; 12(5):943–956. https://doi.org/10.1016/0896-6273(94)90306-9 PMID: 8185953

28. Hudmon A, Schulman H. Neuronal CA2+/calmodulin-dependent protein kinase II: the role of structure and autoregulation in cellular function. Annual review of biochemistry. 2002; 71(1):473–510. https://doi.org/10.1146/annurev.biochem.71.110601.135410 PMID: 12045104

29. Kennedy M, Bennett M, Bulleit R, Erondu N, Jennings V, Miller S, et al. Structure and regulation of type II calcium/calmodulin-dependent protein kinase in central nervous system neurons. In: Cold Spring Harbor symposia on quantitative biology. vol. 55. Cold Spring Harbor Laboratory Press; 1990. p. 101–110.

30. Pepke S, Kinzer-Ursem T, Mihalas S, Kennedy MB. A dynamic model of interactions of Ca2+, calmodulin, and catalytic subunits of Ca2+/calmodulin-dependent protein kinase II. PLoS computational biology. 2010; 6(2):e1000675. https://doi.org/10.1371/journal.pcbi.1000675 PMID: 20168991

31. Colbran RJ. Protein phosphatases and calcium/calmodulin-dependent protein kinase II-dependent synaptic plasticity. Journal of Neuroscience. 2004; 24(39):8404–8409. https://doi.org/10.1523/JNEUROSCI.3602-04.2004 PMID: 15456812

32. Strack S, Choi S, Lovinger DM, Colbran RJ. Translocation of autophosphorylated calcium/calmodulin-dependent protein kinase II to the postsynaptic density. Journal of Biological Chemistry. 1997; 272 (21):13467–13470. https://doi.org/10.1074/jbc.272.21.13467 PMID: 9153188

33. Lisman JE. A mechanism for memory storage insensitive to molecular turnover: a bistable autophosphorylating kinase. Proceedings of the National Academy of Sciences. 1985; 82(9):3055–3057. https://doi.org/10.1073/pnas.82.9.3055

34. Zhabotinsky AM, Camp RN, Epstein IR, Lisman JE. Role of the neurogranin concentrated in spines in the induction of long-term potentiation. Journal of Neuroscience. 2006; 26(28):7337–7347. https://doi.org/10.1523/JNEUROSCI.0729-06.2006 PMID: 16837580

35. Zhabotinsky AM. Bistability in the Ca2+/calmodulin-dependent protein kinase-phosphatase system. Biophysical journal. 2000; 79(5):2211–2221. https://doi.org/10.1016/S0006-3495(00)76469-1 PMID: 11053103

36. Lisman J, Yasuda R, Raghavachari S. Mechanisms of CaMKII action in long-term potentiation. Nature reviews neuroscience. 2012; 13(3):169. https://doi.org/10.1038/nrn3192 PMID: 22334212

37. Lisman JE, Zhabotinsky AM. A model of synaptic memory: a CaMKII/PP1 switch that potentiates transmission by organizing an AMPA receptor anchoring assembly. Neuron. 2001; 31(2):191–201. https://doi.org/10.1016/S0896-6273(01)00364-6 PMID: 11502252

38. Graupner M, Brunel N. STDP in a bistable synapse model based on CaMKII and associated signaling pathways. PLoS computational biology. 2007; 3(11). https://doi.org/10.1371/journal.pcbi.0030221 PMID: 18052535

39. Pharris MC, Bartol TM, Sejnowski TJ, Kennedy MB, Stefan MI, Kinzer-Ursem TL. A multi-state model of the CaMKII dodecamer suggests a role for calmodulin in maintenance of autophosphorylation. 2019.

40. Okamoto H, Ichikawa K. Switching characteristics of a model for biochemical-reaction networks describing autophosphorylation versus dephosphorylation of Ca 2+/calmodulin-dependent protein kinase II. Biological cybernetics. 2000; 82(1):35–47. https://doi.org/10.1007/PL00007960 PMID: 10650906

41. Lengyel I, Voss K, Cammarota M, Bradshaw K, Brent V, Murphy K, et al. Autonomous activity of CaMKII is only transiently increased following the induction of long-term potentiation in the rat hippocampus.

European Journal of Neuroscience. 2004; 20(11):3063–3072. https://doi.org/10.1111/j.1460-9568.2004.03748.x PMID: 15579161

42. Lee SJR, Escobedo-Lozoya Y, Szatmari EM, Yasuda R. Activation of CaMKII in single dendritic spines during long-term potentiation. Nature. 2009; 458(7236):299. https://doi.org/10.1038/nature07842 PMID: 19295602

43. Michalski PJ. First demonstration of bistability in CaMKII, a memory-related kinase. Biophysical journal. 2014; 106(6):1233–1235. https://doi.org/10.1016/j.bpj.2014.01.037 PMID: 24655498

44. Chang JY, Nakahata Y, Hayano Y, Yasuda R. Mechanisms of Ca 2+/calmodulin-dependent kinase II activation in single dendritic spines. Nature communications. 2019; 10(1):1–12. https://doi.org/10.1038/s41467-019-10694-z

45. Linse S, Helmersson A, Forsen S. Calcium binding to calmodulin and its globular domains. Journal of Biological Chemistry. 1991; 266(13):8050–8054. PMID: 1902469

46. Kubota Y, Putkey JA, Waxham MN. Neurogranin controls the spatiotemporal pattern of postsynaptic Ca2+/CaM signaling. Biophysical journal. 2007; 93(11):3848–3859. https://doi.org/10.1529/biophysj.107.106849 PMID: 17704141

47. Persechini A, White HD, Gansz KJ. Different Mechanisms for Ca Dissociation from Complexes of Calmodulin with Nitric Oxide Synthase or Myosin Light Chain Kinase. Journal of Biological Chemistry. 1996; 271(1):62–67. https://doi.org/10.1074/jbc.271.1.62 PMID: 8550626

48. MARTIN SR, MAUNE JF, BECKINGHAM K, BAYLEY PM. Stopped-flow studies of calcium dissociation from calcium-binding-site mutants of Drosophila melanogaster calmodulin. European journal of biochemistry. 1992; 205(3):1107–1117. https://doi.org/10.1111/j.1432-1033.1992.tb16879.x PMID: 1576994

49. Gaertner TR, Putkey JA, Waxham MN. RC3/Neurogranin and Ca2+/calmodulin-dependent protein kinase II produce opposing effects on the affinity of calmodulin for calcium. Journal of Biological Chemistry. 2004; 279(38):39374–39382. https://doi.org/10.1074/jbc.M405352200 PMID: 15262982

50. Peersen OB, Madsen TS, Falke JJ. Intermolecular tuning of calmodulin by target peptides and proteins: differential effects on Ca2+ binding and implications for kinase activation. Protein Science. 1997; 6(4):794–807. https://doi.org/10.1002/pro.5560060406 PMID: 9098889

51. Brown SE, Martin SR, Bayley PM. Kinetic control of the dissociation pathway of calmodulin-peptide complexes. Journal of Biological Chemistry. 1997; 272(6):3389–3397. https://doi.org/10.1074/jbc.272.6.3389 PMID: 9013581

52. Meyer T, Hanson PI, Stryer L, Schulman H. Calmodulin trapping by calcium-calmodulin-dependent protein kinase. Science. 1992; 256(5060):1199–1202. https://doi.org/10.1126/science.256.5060.1199 PMID: 1317063

53. Copeland RA. Enzymes: a practical introduction to structure, mechanism, and data analysis. John Wiley & Sons; 2004.

54. Bradshaw JM, Hudmon A, Schulman H. Chemical quenched flow kinetic studies indicate an intraholoenzyme autophosphorylation mechanism for Ca2+/calmodulin-dependent protein kinase II. Journal of Biological Chemistry. 2002; 277(23):20991–20998. https://doi.org/10.1074/jbc.M202154200 PMID: 11925447

55. Rangamani P, Levy MG, Khan S, Oster G. Paradoxical signaling regulates structural plasticity in dendritic spines. Proceedings of the National Academy of Sciences. 2016; 113(36):E5298–E5307. https://doi.org/10.1073/pnas.1610391113

56. Bradshaw JM, Kubota Y, Meyer T, Schulman H. An ultrasensitive Ca2+/calmodulin-dependent protein kinase II-protein phosphatase 1 switch facilitates specificity in postsynaptic calcium signaling. Proceedings of the National Academy of Sciences. 2003; 100(18):10512–10517. https://doi.org/10.1073/pnas.1932759100

57. Biber A, Schmid G, Hempel K. Calmodulin content in specific brain areas. Experimental brain research. 1984; 56(2):323–326. https://doi.org/10.1007/BF00236287 PMID: 6479265

58. Kakiuchi S, YASUDA S, YAMAZAKI R, TESHIMA Y, KANDA K, KAKIUCHI R, et al. Quantitative determinations of calmodulin in the supernatant and particulate fractions of mammalian tissues. The Journal of Biochemistry. 1982; 92(4):1041–1048. https://doi.org/10.1093/oxfordjournals.jbchem.a134019 PMID: 7174634

59. Watterson D, Harrelson W, Keller P, Sharief F, Vanaman TC. Structural similarities between the Ca2+-dependent regulatory proteins of 3': 5'-cyclic nucleotide phosphodiesterase and actomyosin ATPase. Journal of Biological Chemistry. 1976; 251(15):4501–4513. PMID: 181375

60. Sabatini BL, Oertner TG, Svoboda K. The life cycle of Ca2+ ions in dendritic spines. Neuron. 2002; 33(3):439–452. https://doi.org/10.1016/S0896-6273(02)00573-1 PMID: 11832230

61. Franks KM, Sejnowski TJ. Complexity of calcium signaling in synaptic spines. Bioessays. 2002; 24 (12):1130–1144. https://doi.org/10.1002/bies.10193 PMID: 12447978

62. Yang SN, Tang YG, Zucker RS. Selective induction of LTP and LTD by postsynaptic [Ca2+] i elevation. Journal of neurophysiology. 1999; 81(2):781–787. https://doi.org/10.1152/jn.1999.81.2.781 PMID: 10036277

63. Denk W, Yuste R, Svoboda K, Tank DW. Imaging calcium dynamics in dendritic spines. Current opinion in neurobiology. 1996; 6(3):372–378. https://doi.org/10.1016/S0959-4388(96)80122-X PMID: 8794079

64. Petrozzino JJ, Miller LDP, Connor JA. Micromolar Ca2+ transients in dendritic spines of hippocampal pyramidal neurons in brain slice. Neuron. 1995; 14(6):1223–1231. https://doi.org/10.1016/0896-6273(95)90269-4 PMID: 7605633

65. Bartol TM, Keller DX, Kinney JP, Bajaj CL, Harris KM, Sejnowski TJ, et al. Computational reconstitution of spine calcium transients from individual proteins. Frontiers in synaptic neuroscience. 2015; 7:17. https://doi.org/10.3389/fnsyn.2015.00017 PMID: 26500546

66. Neher E, Augustine G. Calcium gradients and buffers in bovine chromaffin cells. The Journal of physiology. 1992; 450(1):273–301. https://doi.org/10.1113/jphysiol.1992.sp019127 PMID: 1331424

67. Fujii H, Inoue M, Okuno H, Sano Y, Takemoto-Kimura S, Kitamura K, et al. Nonlinear decoding and asymmetric representation of neuronal input information by CaMKII*α* and calcineurin. Cell reports. 2013; 3(4):978–987. https://doi.org/10.1016/j.celrep.2013.03.033 PMID: 23602566

68. Takao K, Okamoto KI, Nakagawa T, Neve RL, Nagai T, Miyawaki A, et al. Visualization of synaptic Ca2+/calmodulin-dependent protein kinase II activity in living neurons. Journal of Neuroscience. 2005; 25(12):3107–3112. https://doi.org/10.1523/JNEUROSCI.0085-05.2005 PMID: 15788767

69. Chang JY, Parra-Bueno P, Laviv T, Szatmari EM, Lee SJR, Yasuda R. Camkii autophosphorylation is necessary for optimal integration of ca 2+ signals during ltp induction, but not maintenance. Neuron. 2017; 94(4):800–808. https://doi.org/10.1016/j.neuron.2017.04.041 PMID: 28521133

70. Johnson T, Bartol T, Sejnowski T, Mjolsness E. Model reduction for stochastic CaMKII reaction kinetics in synapses by graph-constrained correlation dynamics. Physical biology. 2015; 12(4):045005. https://doi.org/10.1088/1478-3975/12/4/045005 PMID: 26086598

71. Tse JK, Giannetti AM, Bradshaw JM. Thermodynamics of calmodulin trapping by Ca2+/calmodulin-dependent protein kinase II: Subpicomolar K d determined using competition titration calorimetry. Biochemistry. 2007; 46(13):4017–4027. https://doi.org/10.1021/bi700013y PMID: 17352496

72. Michalski P. The Delicate Bistability of CaMKII. Biophysical Journal. 2013; 105:794–806. https://doi.org/10.1016/j.bpj.2013.06.038 PMID: 23931327

73. Miller P, Zhabotinsky AM, Lisman JE, Wang XJ. The stability of a stochastic CaMKII switch: dependence on the number of enzyme molecules and protein turnover. PLoS biology. 2005; 3(4). https://doi.org/10.1371/journal.pbio.0030107

74. Singh D, Bhalla US. Subunit exchange enhances information retention by CaMKII in dendritic spines. Elife. 2018; 7:e41412. https://doi.org/10.7554/eLife.41412 PMID: 30418153

75. Rakhilin S, Olson P, Nishi A, Starkova N, Fienberg A, Nairn A, et al. A network of control mediated by regulator of calcium/calmodulin-dependent signaling. Science. 2004; 306(5696):698–701. https://doi.org/10.1126/science.1099961 PMID: 15499021

76. Nair AG, Bhalla US, Kotaleski JH. Role of DARPP-32 and ARPP-21 in the emergence of temporal constraints on striatal calcium and dopamine integration. PLoS computational biology. 2016; 12(9). https://doi.org/10.1371/journal.pcbi.1005080 PMID: 27584878

77. Pak JH, Huang FL, Li J, Balschun D, Reymann KG, Chiang C, et al. Involvement of neurogranin in the modulation of calcium/calmodulin-dependent protein kinase II, synaptic plasticity, and spatial learning: a study with knockout mice. Proceedings of the National Academy of Sciences. 2000; 97(21):11232–11237. https://doi.org/10.1073/pnas.210184697

78. Krucker T, Siggins GR, McNamara RK, Lindsley KA, Dao A, Allison DW, et al. Targeted disruption of RC3 reveals a calmodulin-based mechanism for regulating metaplasticity in the hippocampus. Journal of Neuroscience. 2002; 22(13):5525–5535. https://doi.org/10.1523/JNEUROSCI.22-13-05525.2002 PMID: 12097504

79. Díez-Guerra FJ. Neurogranin, a link between calcium/calmodulin and protein kinase C signaling in synaptic plasticity. IUBMB life. 2010; 62(8):597–606. https://doi.org/10.1002/iub.357 PMID: 20665622

80. Zhong L, Cherry T, Bies CE, Florence MA, Gerges NZ. Neurogranin enhances synaptic strength through its interaction with calmodulin. The EMBO journal. 2009; 28(19):3027–3039. https://doi.org/10.1038/emboj.2009.236 PMID: 19713936

81. Wang JH, Kelly PT. Postsynaptic injection of CA2+/CaM induces synaptic potentiation requiring CaMKII and PKC activity. Neuron. 1995; 15(2):443–452. https://doi.org/10.1016/0896-6273(95)90048-9 PMID: 7646896

82. Colgan LA, Hu M, Misler JA, Parra-Bueno P, Moran CM, Leitges M, et al. PKCα integrates spatiotemporally distinct Ca 2+ and autocrine BDNF signaling to facilitate synaptic plasticity. Nature neuroscience. 2018; 21(8):1027–1037. https://doi.org/10.1038/s41593-018-0184-3 PMID: 30013171

83. Urakubo H, Sato M, Ishii S, Kuroda S. In vitro reconstitution of a CaMKII memory switch by an NMDA receptor-derived peptide. Biophysical journal. 2014; 106(6):1414–1420. https://doi.org/10.1016/j.bpj.2014.01.026 PMID: 24655517

84. Hayashi Y, Shi SH, Esteban JA, Piccini A, Poncer JC, Malinow R. Driving AMPA receptors into synapses by LTP and CaMKII: requirement for GluR1 and PDZ domain interaction. Science. 2000; 287 (5461):2262–2267. https://doi.org/10.1126/science.287.5461.2262 PMID: 10731148

85. Coultrap SJ, Freund RK, O'Leary H, Sanderson JL, Roche KW, Dell'Acqua ML, et al. Autonomous CaMKII mediates both LTP and LTD using a mechanism for differential substrate site selection. Cell reports. 2014; 6(3):431–437. https://doi.org/10.1016/j.celrep.2014.01.005 PMID: 24485660

86. Opazo P, Labrecque S, Tigaret CM, Frouin A, Wiseman PW, De Koninck P, et al. CaMKII triggers the diffusional trapping of surface AMPARs through phosphorylation of stargazin. Neuron. 2010; 67 (2):239–252. https://doi.org/10.1016/j.neuron.2010.06.007 PMID: 20670832

87. Xie Z, Srivastava DP, Photowala H, Kai L, Cahill ME, Woolfrey KM, et al. Kalirin-7 controls activity-dependent structural and functional plasticity of dendritic spines. Neuron. 2007; 56(4):640–656. https://doi.org/10.1016/j.neuron.2007.10.005 PMID: 18031682

88. Fleming IN, Elliott CM, Exton JH. Phospholipase C-γ, protein kinase C and Ca2+/calmodulin-dependent protein kinase II are involved in platelet-derived growth factor-induced phosphorylation of Tiam1. FEBS letters. 1998; 429(3):229–233. https://doi.org/10.1016/S0014-5793(98)00566-3 PMID: 9662423

89. Tolias KF, Bikoff JB, Burette A, Paradis S, Harrar D, Tavazoie S, et al. The Rac1-GEF Tiam1 couples the NMDA receptor to the activity-dependent development of dendritic arbors and spines. Neuron. 2005; 45(4):525–538. https://doi.org/10.1016/j.neuron.2005.01.024 PMID: 15721239

90. Carlisle HJ, Manzerra P, Marcora E, Kennedy MB. SynGAP regulates steady-state and activity-dependent phosphorylation of cofilin. Journal of Neuroscience. 2008; 28(50):13673–13683. https://doi.org/10.1523/JNEUROSCI.4695-08.2008 PMID: 19074040

91. Hoffman L, Farley MM, Waxham MN. Calcium-calmodulin-dependent protein kinase II isoforms differentially impact the dynamics and structure of the actin cytoskeleton. Biochemistry. 2013; 52(7):1198–1207. https://doi.org/10.1021/bi3016586 PMID: 23343535

92. Khan S, Conte I, Carter T, Bayer KU, Molloy JE. Multiple CaMKII binding modes to the actin cytoskeleton revealed by single-molecule imaging. Biophysical journal. 2016; 111(2):395–408. https://doi.org/10.1016/j.bpj.2016.06.007 PMID: 27463141

93. Sanabria H, Swulius MT, Kolodziej SJ, Liu J, Waxham MN. βCaMKII regulates actin assembly and structure. Journal of Biological Chemistry. 2009; 284(15):9770–9780. https://doi.org/10.1074/jbc.M809518200 PMID: 19208632

94. Zhu JJ, Qin Y, Zhao M, Van Aelst L, Malinow R. Ras and Rap control AMPA receptor trafficking during synaptic plasticity. Cell. 2002; 110(4):443–455. https://doi.org/10.1016/S0092-8674(02)00897-8 PMID: 12202034

95. Opazo P, Choquet D. A three-step model for the synaptic recruitment of AMPA receptors. Molecular and Cellular Neuroscience. 2011; 46(1):1–8. https://doi.org/10.1016/j.mcn.2010.08.014 PMID: 20817097

96. Appleby VJ, Corrêa SA, Duckworth JK, Nash JE, Noël J, Fitzjohn SM, et al. LTP in hippocampal neurons is associated with a CaMKII-mediated increase in GluA1 surface expression. Journal of neurochemistry. 2011; 116(4):530–543. https://doi.org/10.1111/j.1471-4159.2010.07133.x PMID: 21143596

97. Barria A, Muller D, Derkach V, Griffith LC, Soderling TR. Regulatory phosphorylation of AMPA-type glutamate receptors by CaM-KII during long-term potentiation. Science. 1997; 276(5321):2042–2045. https://doi.org/10.1126/science.276.5321.2042 PMID: 9197267

98. Benke TA, Lüthi A, Isaac JT, Collingridge GL. Modulation of AMPA receptor unitary conductance by synaptic activity. Nature. 1998; 393(6687):793. https://doi.org/10.1038/31709 PMID: 9655394

99. Lee HK, Barbarosie M, Kameyama K, Bear MF, Huganir RL. Regulation of distinct AMPA receptor phosphorylation sites during bidirectional synaptic plasticity. Nature. 2000; 405(6789):955. https://doi.org/10.1038/35016089 PMID: 10879537

100. Krapivinsky G, Medina I, Krapivinsky L, Gapon S, Clapham DE. SynGAP-MUPP1-CaMKII synaptic complexes regulate p38 MAP kinase activity and NMDA receptor-dependent synaptic AMPA receptor potentiation. Neuron. 2004; 43(4):563–574. https://doi.org/10.1016/j.neuron.2004.08.003 PMID: 15312654

101. Pi HJ, Otmakhov N, El Gaamouch F, Lemelin D, De Koninck P, Lisman J. CaMKII control of spine size and synaptic strength: role of phosphorylation states and nonenzymatic action. Proceedings of the National Academy of Sciences. 2010; 107(32):14437–14442. https://doi.org/10.1073/pnas.1009268107

102. Asrican B, Lisman J, Otmakhov N. Synaptic Strength of Individual Spines Correlates with Bound Ca2+–Calmodulin-Dependent Kinase II. Journal of Neuroscience. 2007; 27(51):14007–14011. https://doi.org/10.1523/JNEUROSCI.3587-07.2007 PMID: 18094239

103. Barcomb K, Hell JW, Benke TA, Bayer KU. The CaMKII/GluN2B protein interaction maintains synaptic strength. Journal of Biological Chemistry. 2016; 291(31):16082–16089. https://doi.org/10.1074/jbc.M116.734822 PMID: 27246855

104. Bi Gq, Poo Mm. Synaptic modifications in cultured hippocampal neurons: dependence on spike timing, synaptic strength, and postsynaptic cell type. Journal of neuroscience. 1998; 18(24):10464–10472. https://doi.org/10.1523/JNEUROSCI.18-24-10464.1998 PMID: 9852584

105. Bhattacharyya RP, Reményi A, Good MC, Bashor CJ, Falick AM, Lim WA. The Ste5 scaffold allosterically modulates signaling output of the yeast mating pathway. Science. 2006; 311(5762):822–826. https://doi.org/10.1126/science.1120941 PMID: 16424299

106. Kolch W. Coordinating ERK/MAPK signalling through scaffolds and inhibitors. Nature reviews Molecular cell biology. 2005; 6(11):827. https://doi.org/10.1038/nrm1743 PMID: 16227978

107. Locasale JW, Shaw AS, Chakraborty AK. Scaffold proteins confer diverse regulatory properties to protein kinase cascades. Proceedings of the National Academy of Sciences. 2007; 104(33):13307–13312. https://doi.org/10.1073/pnas.0706311104

108. Ohadi D, Rangamani P. Geometric control of frequency modulation of cAMP oscillations due to Ca2+-bursts in dendritic spines. bioRxiv. 2019; p. 520643.

109. Oliveira RF, Terrin A, Di Benedetto G, Cannon RC, Koh W, Kim M, et al. The role of type 4 phosphodiesterases in generating microdomains of cAMP: large scale stochastic simulations. PloS one. 2010; 5(7):e11725. https://doi.org/10.1371/journal.pone.0011725 PMID: 20661441

110. Bell M, Bartol T, Sejnowski T, Rangamani P. Addendum: Dendritic spine geometry and spine apparatus organization govern the spatiotemporal dynamics of calcium. The Journal of general physiology. 2019; 151(9):2221. https://doi.org/10.1085/jgp.20181226107312019a PMID: 31375548

111. Ohadi D, Schmitt DL, Calabrese B, Halpain S, Zhang J, Rangamani P. Computational modeling reveals frequency modulation of calcium-cAMP/PKA pathway in dendritic spines. bioRxiv. 2019; p. 521740.

112. Cugno A, Bartol TM, Sejnowski TJ, Iyengar R, Rangamani P. Geometric principles of second messenger dynamics in dendritic spines. Scientific reports. 2019; 9(1):1–18. https://doi.org/10.1038/s41598-019-48028-0

113. Khan S, Downing KH, Molloy JE. Architectural Dynamics of CaMKII-Actin Networks. Biophysical journal. 2019; 116(1):104–119. https://doi.org/10.1016/j.bpj.2018.11.006 PMID: 30527447

114. Coultrap SJ, Bayer KU. CaMKII regulation in information processing and storage. Trends in neurosciences. 2012; 35(10):607–618. https://doi.org/10.1016/j.tins.2012.05.003 PMID: 22717267

115. Myers JB, Zaegel V, Coultrap SJ, Miller AP, Bayer KU, Reichow SL. The CaMKII holoenzyme structure in activation-competent conformations. Nature communications. 2017; 8:15742. https://doi.org/10.1038/ncomms15742 PMID: 28589927

116. Harris LA, Hogg JS, Tapia JJ, Sekar JA, Gupta S, Korsunsky I, et al. BioNetGen 2.2: advances in rule-based modeling. Bioinformatics. 2016; 32(21):3366–3368. https://doi.org/10.1093/bioinformatics/btw469 PMID: 27402907

117. Faeder JR, Blinov ML, Hlavacek WS. Rule-based modeling of biochemical systems with 26 BioNetGen. In: Systems biology. Springer; 2009. p. 113–167.

118. Blinov ML, Faeder JR, Goldstein B, Hlavacek WS. BioNetGen: software for rule-based modeling of signal transduction based on the interactions of molecular domains. Bioinformatics. 2004; 20(17):3289–3291. https://doi.org/10.1093/bioinformatics/bth378 PMID: 15217809

119. Sneddon MW, Faeder JR, Emonet T. Efficient modeling, simulation and coarse-graining of biological complexity with NFsim. Nature methods. 2011; 8(2):177. https://doi.org/10.1038/nmeth.1546 PMID: 21186362

120. Tapia JJ, Saglam AS, Czech J, Kuczewski R, Bartol TM, Sejnowski TJ, et al. MCell-R: A particle-resolution network-free spatial modeling framework. In: Modeling Biomolecular Site Dynamics. Springer; 2019. p. 203–229.